Computational Environments for Coupling Multiphase Flow, Transport, and Geomechanics in Modeling Carbon Sequestration in Saline Aquifers

Mary Fanett Wheeler

Center for Subsurface Modeling
Institute for Computation Engineering and Sciences
The University of Texas at Austin

Acknowledge

- Collaborators:
  - Algorithms: UT-Austin (T. Arbogast, M. Delshad, E. Gildin, G. Pencheva, S. Thomas, T. Wildey, G. Xue, C. Yuan): Pitt (I. Yotov); ConocoPhillips (H. Klie), Paris VI (V. Girault, M. Vohralik); Clemson (S. Sun)
  - Parallel Computation: IBM (K. Jordan); Rutgers (M. Parashar)
  - Closed Loop Optimization: NI (I. Alvarado, D. Schmidt)
  - Phase Behaviour and Compositional Modeling : UT-Austin (M. Delshad); Yale (A. Firoozabadi)
  - Support of Projects: NSF, DOE, KAUST, and Industrial Affiliates (Aramco, BP, Chevron, ConocoPhillips, ExxonMobil, IBM)

Outline

- Motivation
  - Why Carbon Capture and Storage (CCS)?
  - Carbon Sequestration Storage Options
- Mathematical and Computational Models – Objectives and Present Capabilities
- Mathematical and Computational Challenges
  - Discretizations (see Pencheva, Thomas & Xue lectures)
  - Solvers (see Wildey lecture)
  - Multiscale and Uncertainty Quantification
  - A Posteriori Error Estimates and Adaptivity
  - Closed Loop Optimization
- Summary

World Primary Energy Demand

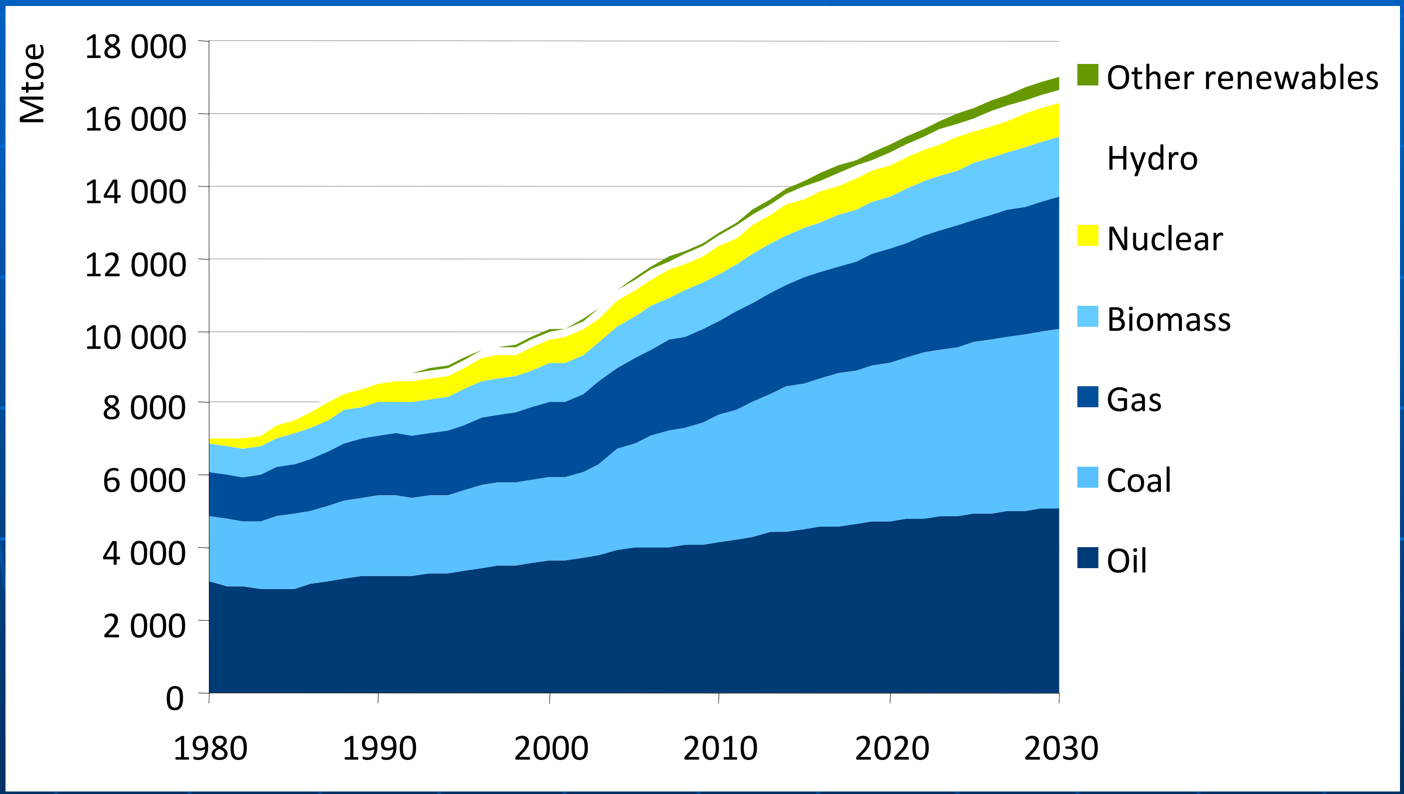

From: Joan MacNaughton (Alstom Power Company)

World energy demand expands by 45% between now and 2030 – an average rate of increase of 1.6% per year – with coal accounting for more than a third of the overall rise

World Oil Production by Source

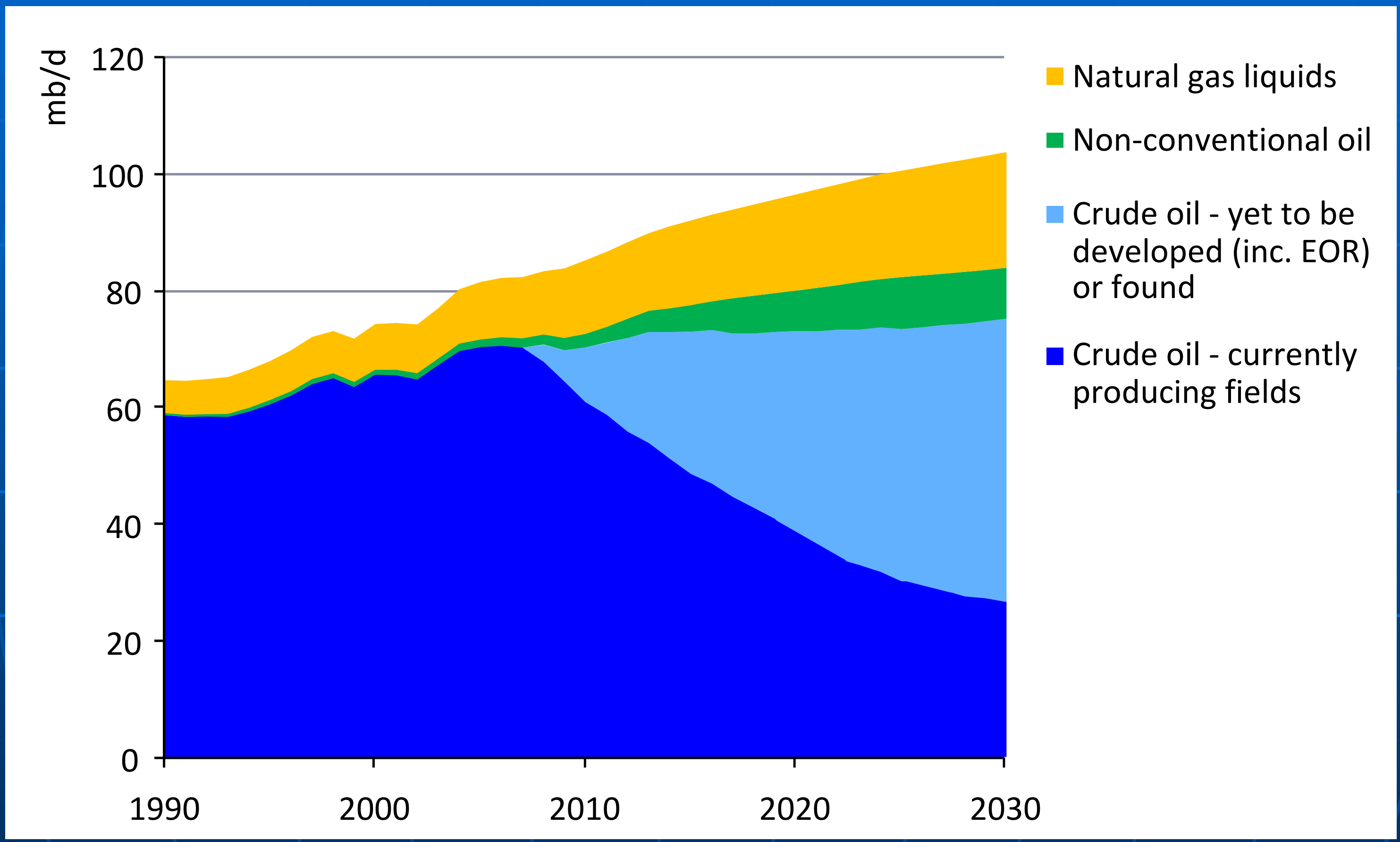

From: Joan MacNaughton (Alstom Power Company)

Even if oil demand was to remain flat to 2030, 45 mb/d of gross capacity – roughly four times the capacity of Saudi Arabia – would be needed just to offset decline from existing oilfields

CO2 from Fossil Fuel Combustion

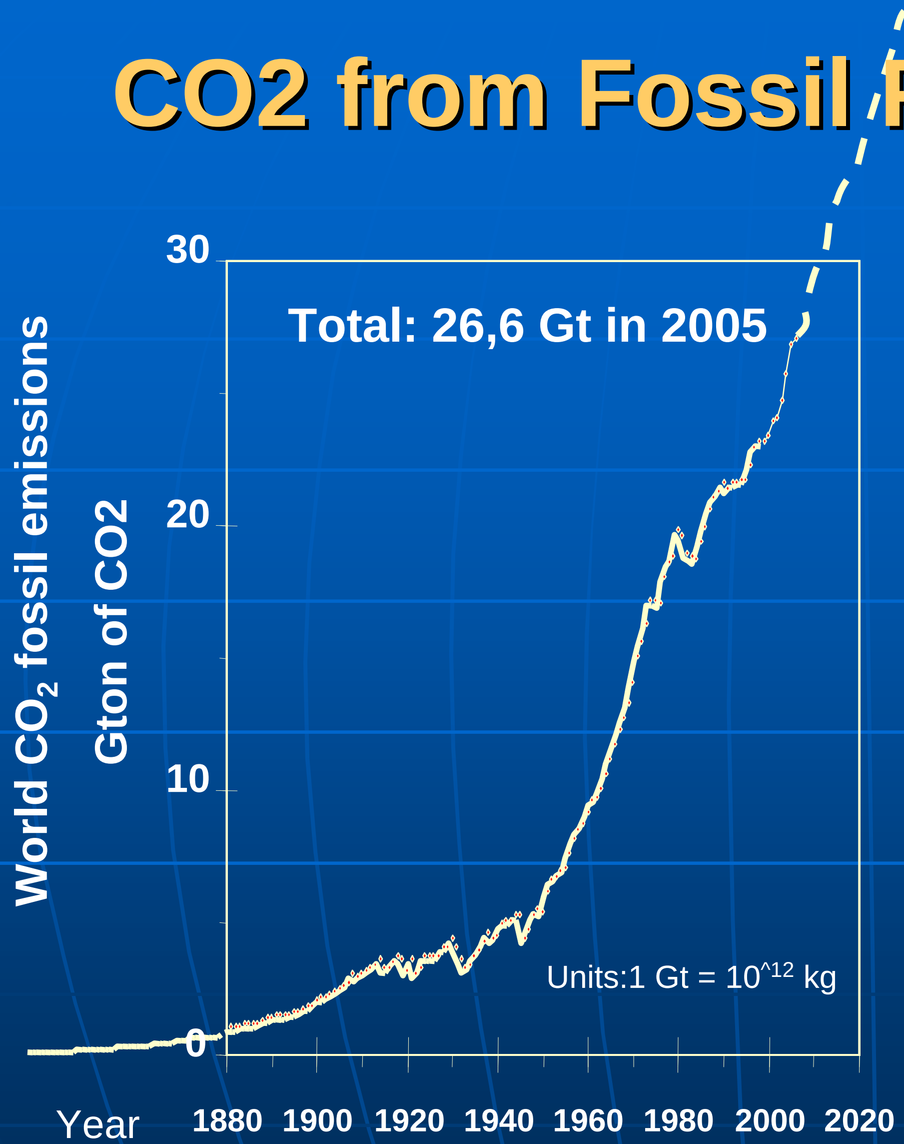

Source: Alstom, adapted from CDIAC 2004

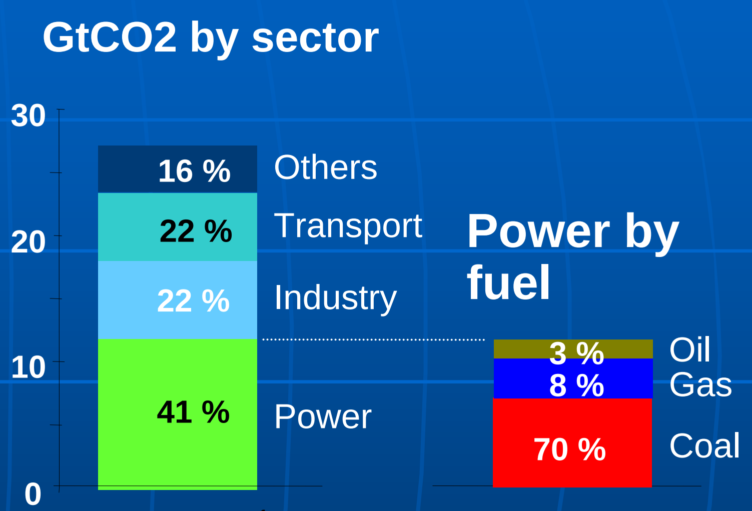

Source: IEA/OECD (2001)

From: Joan MacNaughton (Alstom Power Company)

Coal generates 70% of the CO_2 emissions from power generation

CO_2 Storage Options

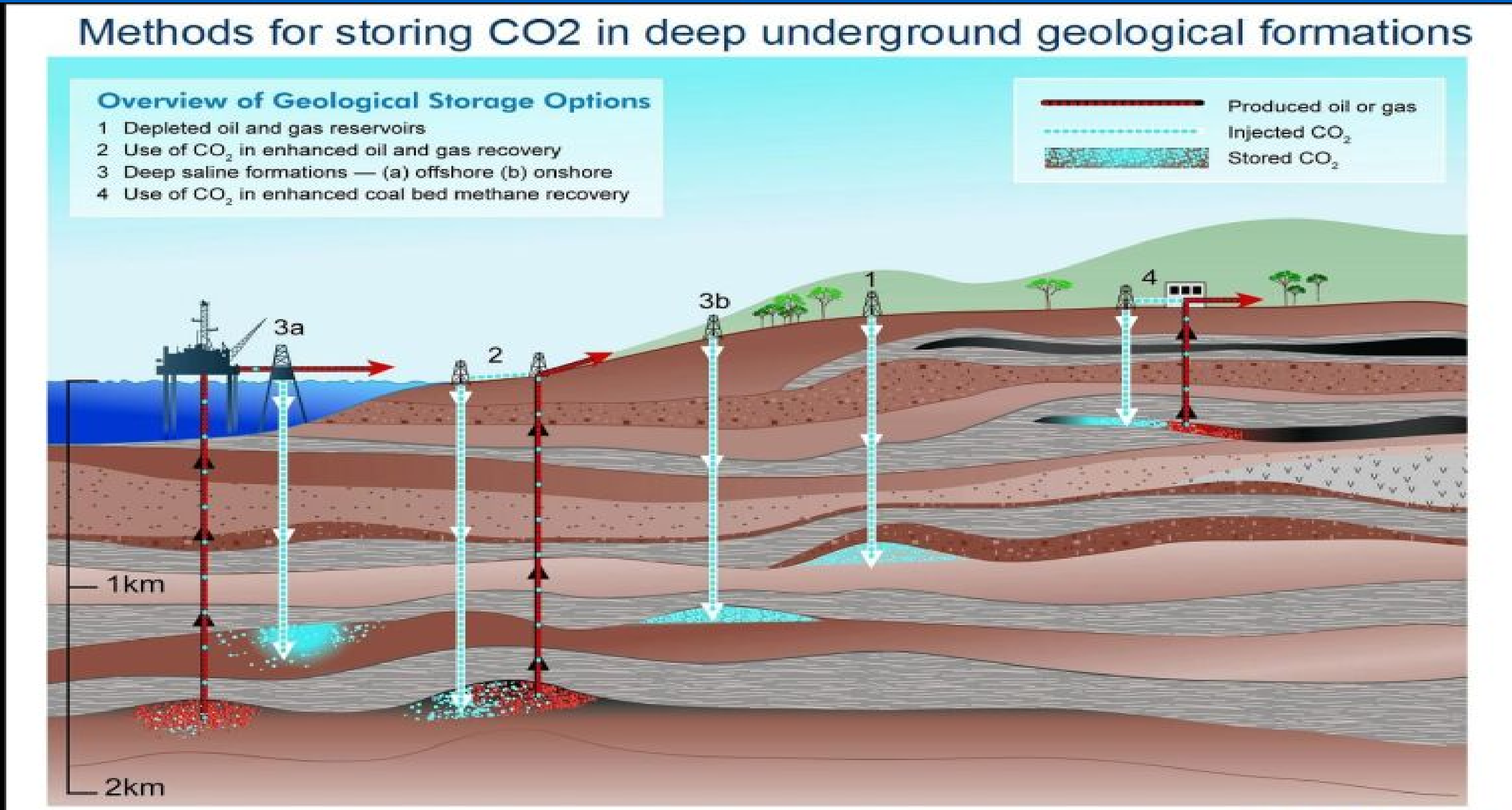

SRCCS Figure TS-7

Global Experience in CO_2 Injection

From: Peter Cook, CO2CRC

Planned Commercial Projects

- ✓ Snohvit- Norway (2008) -Aquifer
- ✓ Gorgon- Australia (2008-2010) - Aquifer
- ✓ Miller-Peterhead - UK (2009) - EOR
- ✓ Carson - US (2009) – Oil/gas reservoirs
- ✓ Draugen – Norway (2010) - EOR

Total CO2 stored ~ 12.5 MT CO_2 / yr

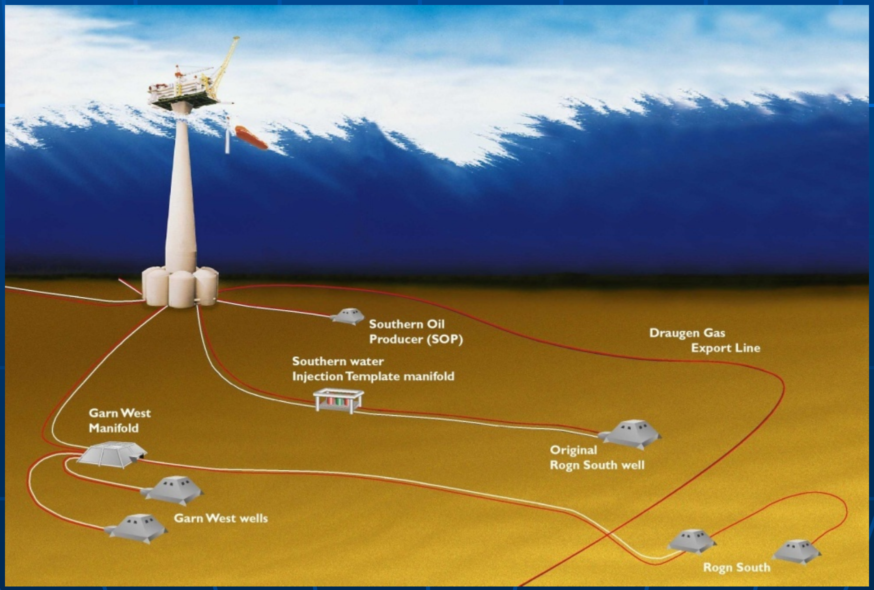

CO_2 Injection and Trapping Mechanisms

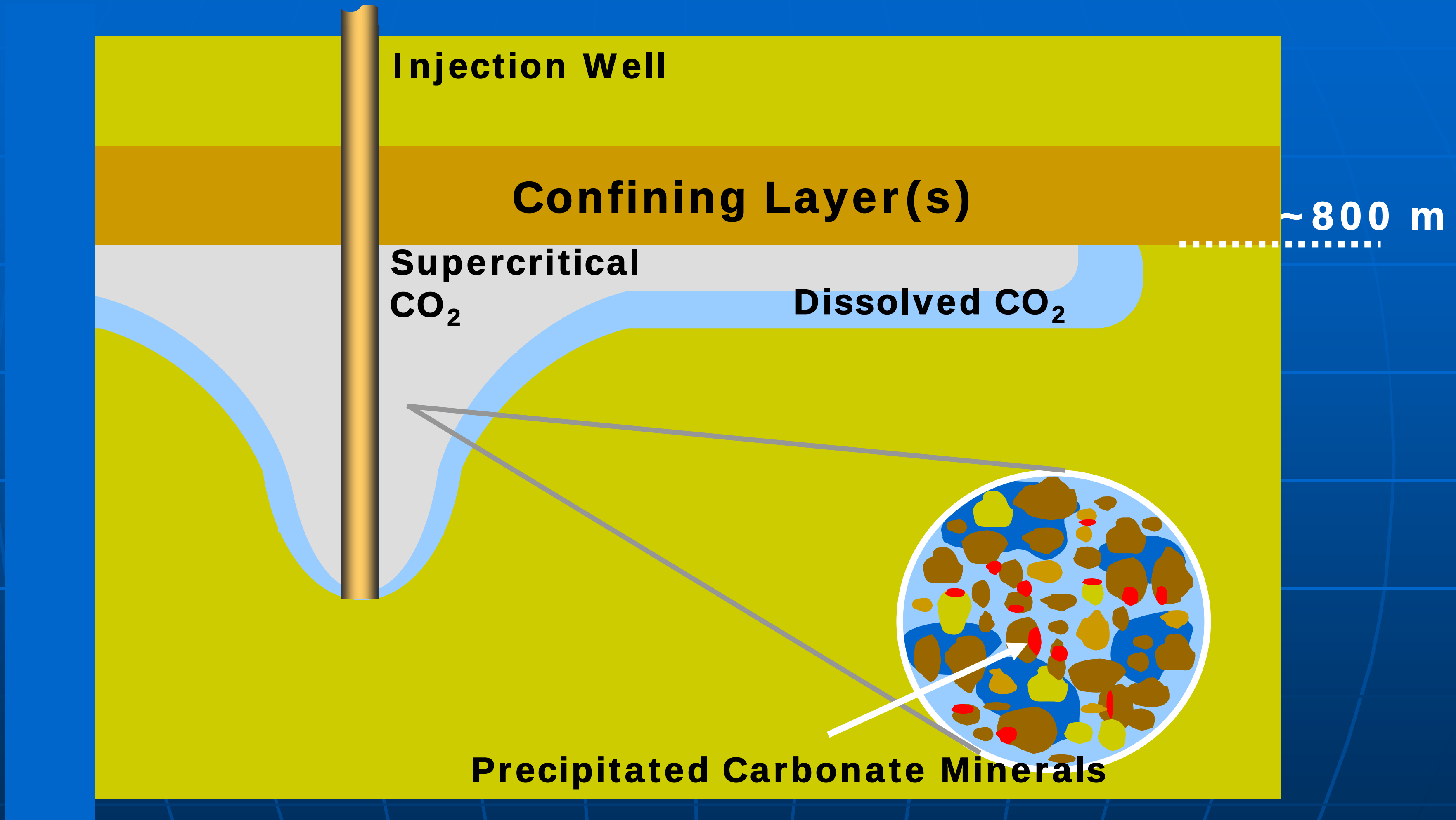

Stratigraphic Trapping | Solubility Trapping | Hydrodynamic Trapping | Mineral Trapping

Celia et al, 2002

Effect of Geology on CO_2 Migration

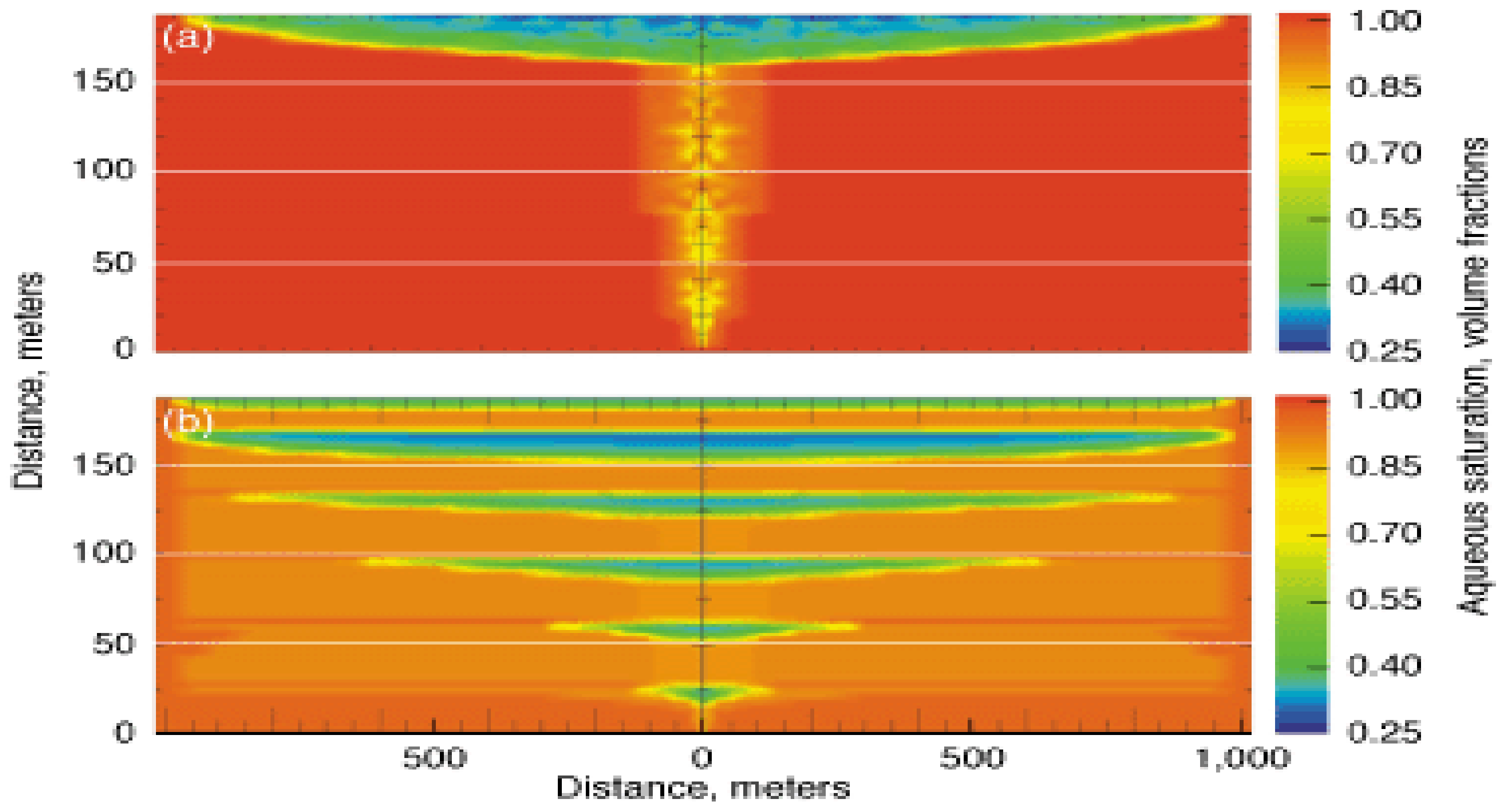

Sequestration performance depends on the geology of the proposed sequestration site. (a) In an aquifer with no shale layers, the CO_2 plume rises quickly to the aquifer caprock, where it migrates laterally beneath this impermeable seal. (b) When shale units are present, they effectively retard the plume's vertical migration while promoting its lateral extension, thus enhancing the effects of solubility and mineral trapping.

GCEP: Stanford

Key Issues in CO_2 Storage

- What is the likelihood and magnitude of CO_2 leakage and what are the environmental impacts?
- How effective are different CO_2 trapping mechanisms?
- What physical, geochemical, and geomechanical processes are important for the next few centuries and how these processes impact the storage efficacy and security?
- What are the necessary models and modeling capabilities to assess the fate of injected CO_2?
- What are the computational needs and capabilities to address these issues?
- How these tools can be made useful and accessible to regulators and industry?

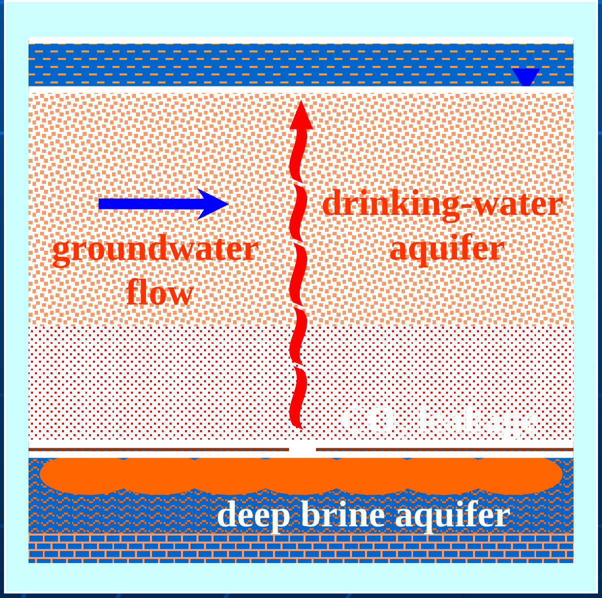

CO_2 Sequestration Modeling Approach

- **Numerical simulation**
  - ✓ Characterization (fault, fractures)
  - ✓ Appropriate gridding
  - ✓ Compositional EOS
  - ✓ Parallel computing capability
- **Key processes**
  - ✓ CO_2/brine mass transfer
  - ✓ Multiphase flow
    - ✓ During injection *(pressure driven)*
    - ✓ After injection *(gravity driven)*
  - ✓ Geochemical reactions
  - ✓ Geomechanical modeling

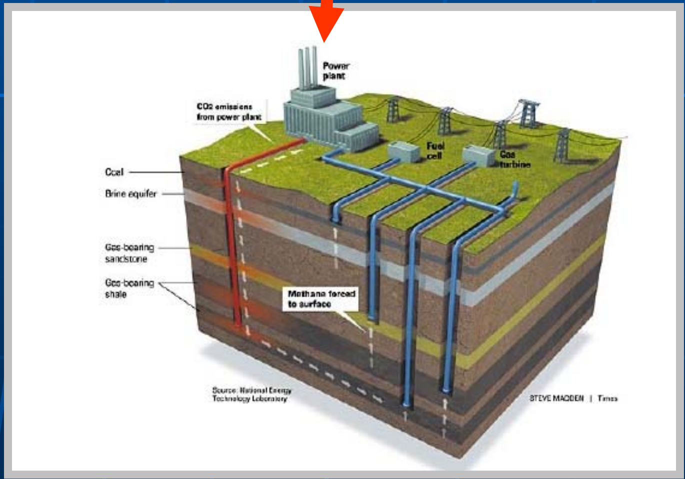

Compositional Modeling

Figure 1 CO_2 phase diagram (based on Atkins, 1982).

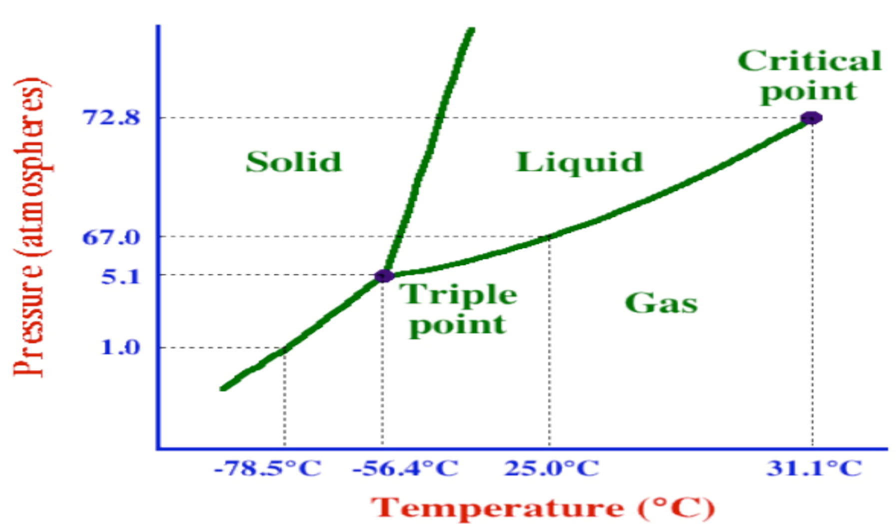

Figure 15 Comparison of CO_2 solubility data for a range of salinities.

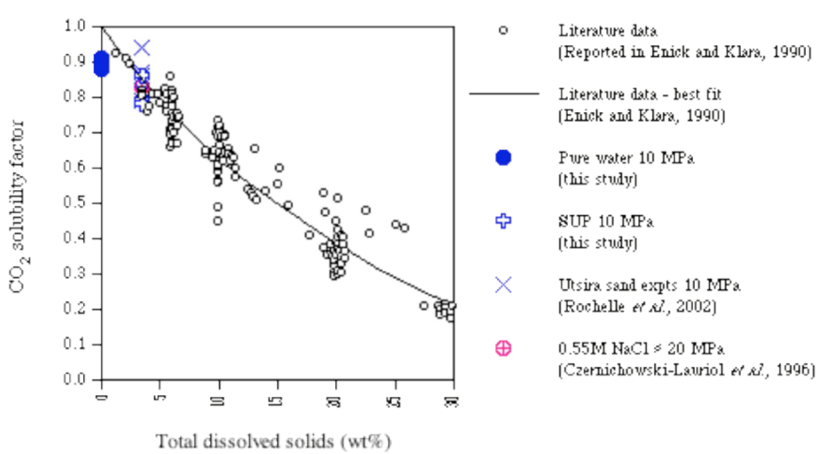

Figure 3 Measured solubility of CO_2 in distilled de-ionised water at 8 MPa.

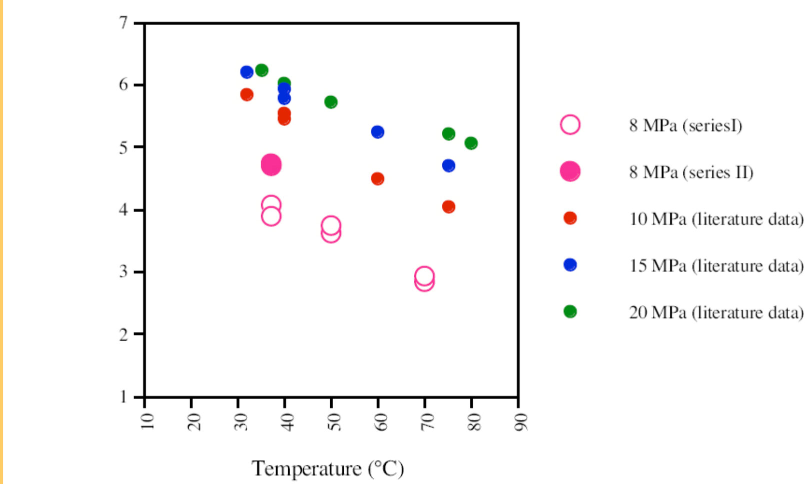

Objectives

- Accurate physic-based simulation of CO_2 storage
- Incorporate realistic phase behavior and physical property model enhancements
- Include geochemical, geomechanical, and geobiological couplings with flow to investigate their impact at different time scales
- Implementation of efficient and accurate parallel multiscale and multiphysics algorithms based on accurate adaptive error estimators
- Train students and postdocs on above collaborative projects

IPARS-COMP Flow Equations

Mass Balance Equation

$$\frac{\partial\left(\phi N_i\right)}{\partial t}+\nabla.\left(\sum_{\alpha}\rho_{\alpha}\xi_i^{\alpha}u_{\alpha}-\phi\rho_{\alpha}S_{\alpha}D_i^{\alpha}\nabla\xi_i^{\alpha}\right)=q_i$$

Pressure Equation

$$\frac{\partial S_T}{\partial p}\delta p+\sum_i\frac{\partial S_T}{\partial N_i}\delta N_i+\sum_i\frac{\partial S_T}{\partial \ln K_i}\delta(\ln K_i)=1-S_T^k.$$

Solution Method

- Iteratively coupled until a volume balance convergence criterion is met or a maximum number of iterations exceeded.

Thermal & Chemistry Equations

Energy Balance

- ✓ Solved using a time-split scheme (operator splitting)
- ✓ Higher-order Godunov for advection
- ✓ Fully implicit/explicit in time and Mixed FEM in space for thermal conduction

$$\frac{\partial(M_T T)}{\partial t} + \nabla.\left(\sum_\alpha \rho_\alpha C_{p\alpha} u_\alpha T - \lambda \nabla T\right) = q_H$$

$$\text{Internal energy}: M_T$$

$$M_T = (1-\phi)\rho_s C_{vs} + \phi \sum_\alpha \rho_\alpha C_{v\alpha} S_\alpha$$

Chemistry

- ✓ System of (non-linear) ODEs
- ✓ Solved using a higher order integration schemes such as Runge-Kutta methods

$$\frac{d\mathbf{c}}{dt} = \mathbf{r}(\mathbf{c}).$$

$$\mathbf{k}_{1,i} = \Delta\tau^l \mathbf{r}_i(\mathbf{c})$$

$$\mathbf{k}_{2,i} = \Delta\tau^l \mathbf{r}_i\left(\mathbf{c} + \frac{1}{2}\mathbf{k}_1\right)$$

$$\hat{\mathbf{c}} = \mathbf{c} + \mathbf{k}_2.$$

EOS Model

Peng-Robinson EOS

$$P_\alpha = \frac{RT}{v_\alpha - b_\alpha} - \frac{a_\alpha(T)}{v_\alpha(v_\alpha + b_\alpha) + b_\alpha(v_\alpha - b_\alpha)}$$

CO_2 Properties

Fugacity (*T*, *P*)

Density (*T*, *P*)

Viscosity (*T*, *P*)

Aqueous Solution Properties

CO_2 Solubility (*T*, *P*)

Aqueous Density (*T*, *P*)

Effect of salinity

Coupled Flow-Thermal-Chemistry Algorithm

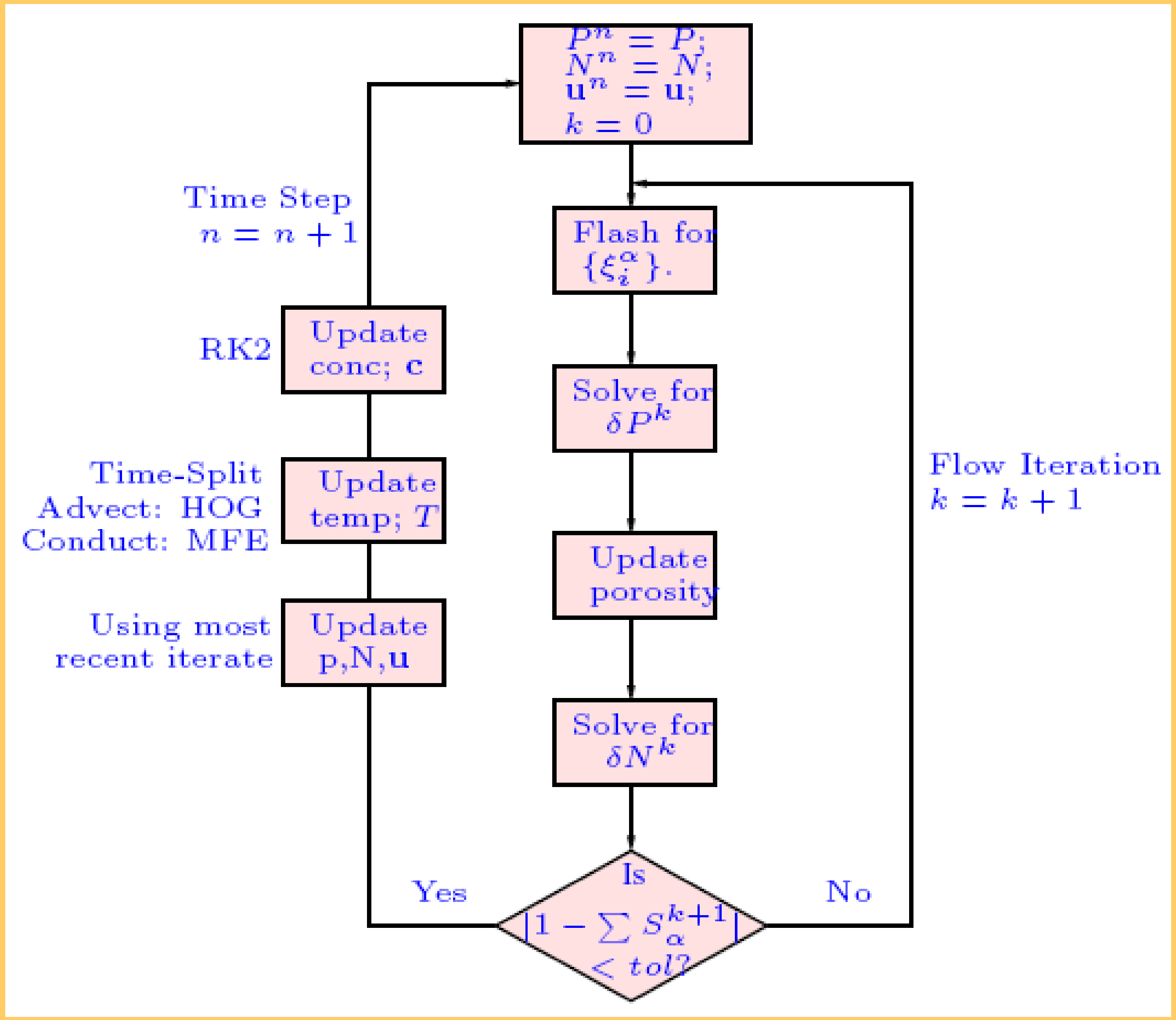

CO2 EOR Simulations

Verification

SPE5 -- A quarter of 5 spot benchmark WAG problem
3-phase, 6 components C1, C3, C6, C10, C15, C20

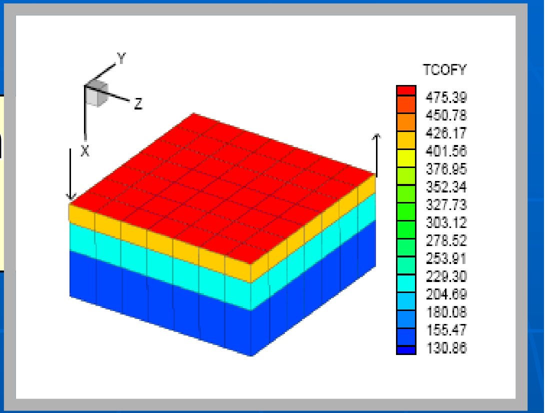

IPARS-COMP vs CMG-GEM

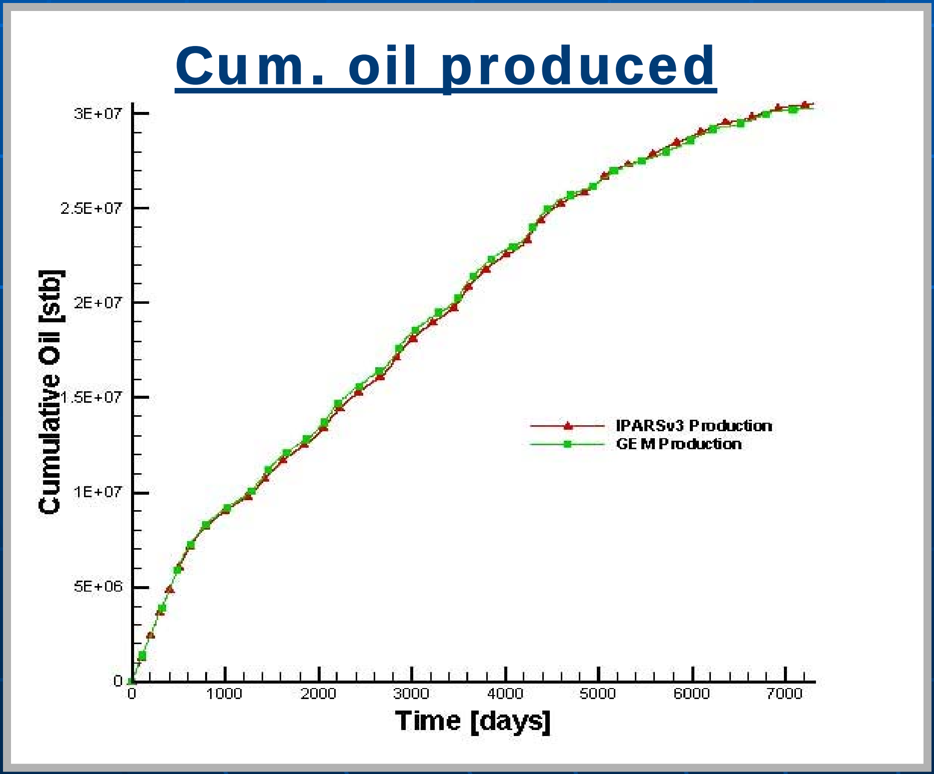

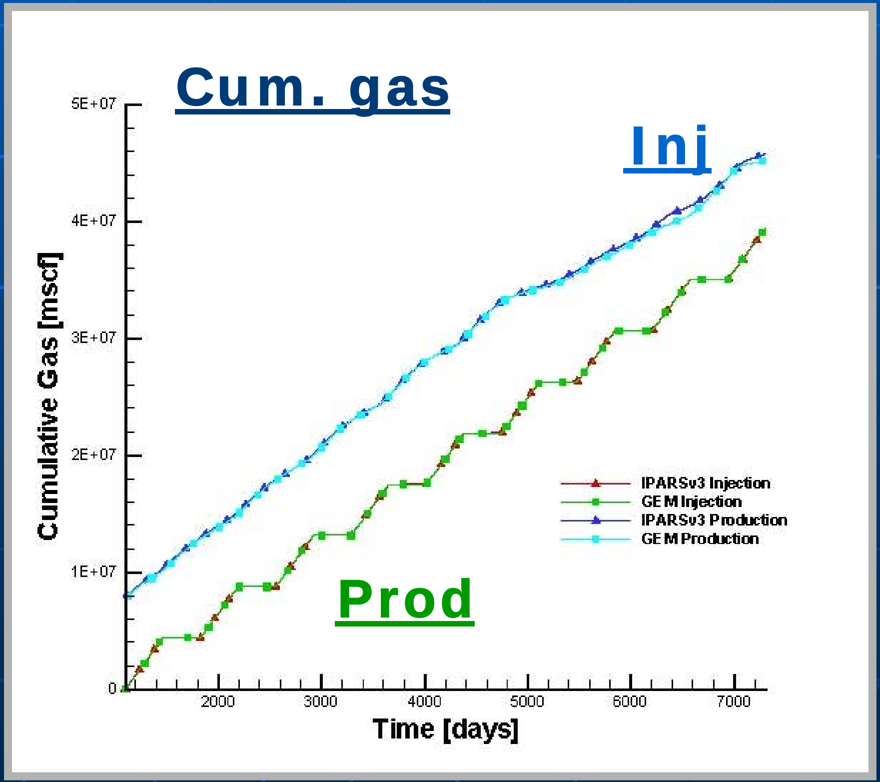

Verification

CO_2 pattern flood injection

3-phase, 10 components CO_2, N_2, C1, C3, C4, C5, C6, C15, C20

IPARS-COMP vs CMG-GEM

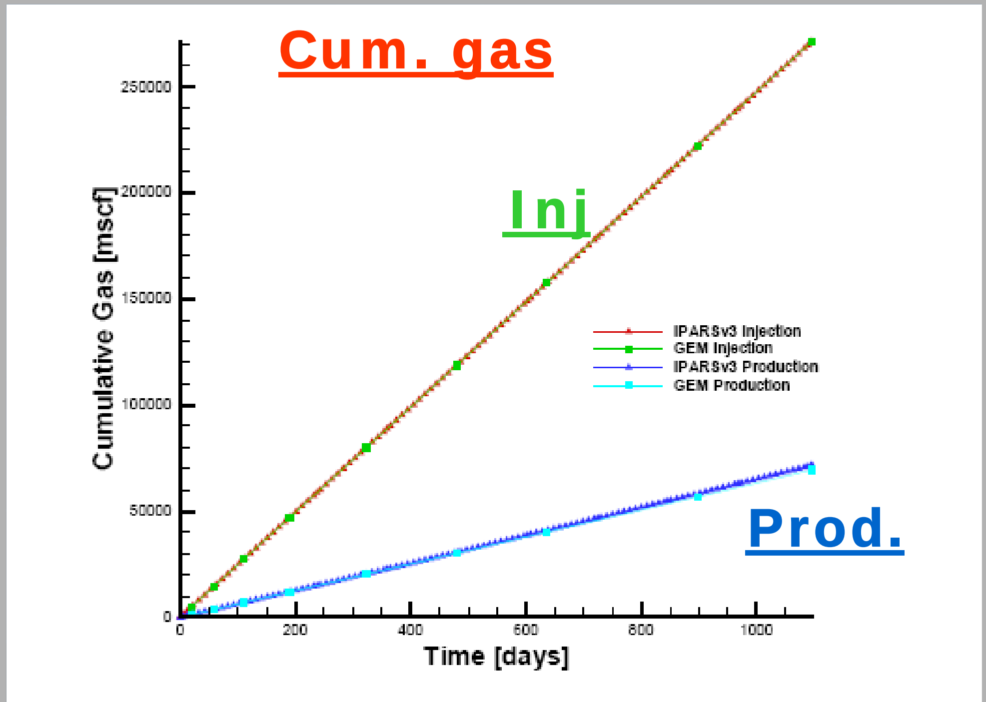

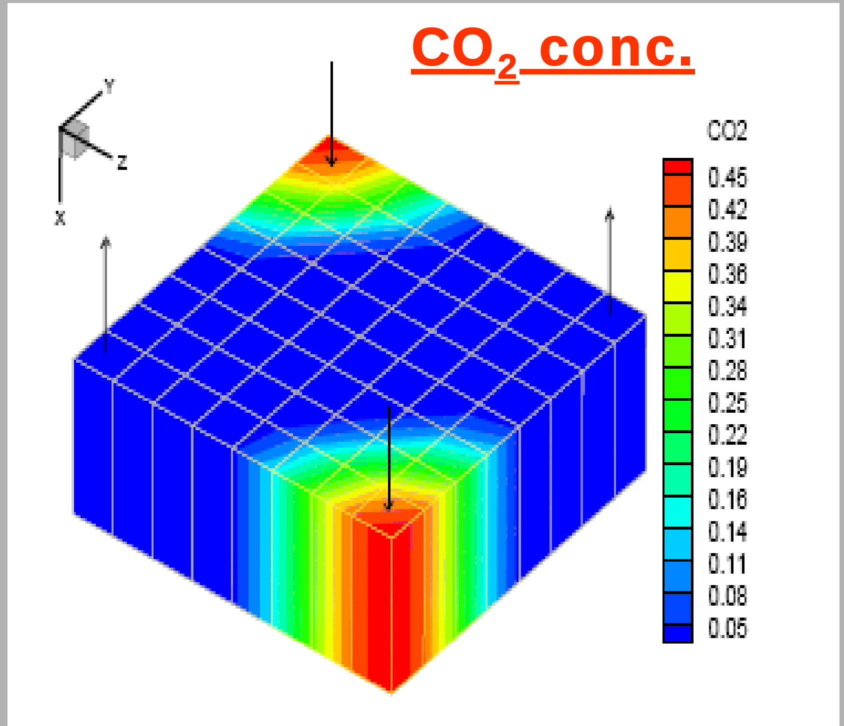

Parallel Simulations

Modified SPE5 WAG injection

- **Permeability from SPE10**
- **160x160x40 (1,024,000 cells)**
- **32, 64, 128, 256, 512 processors**

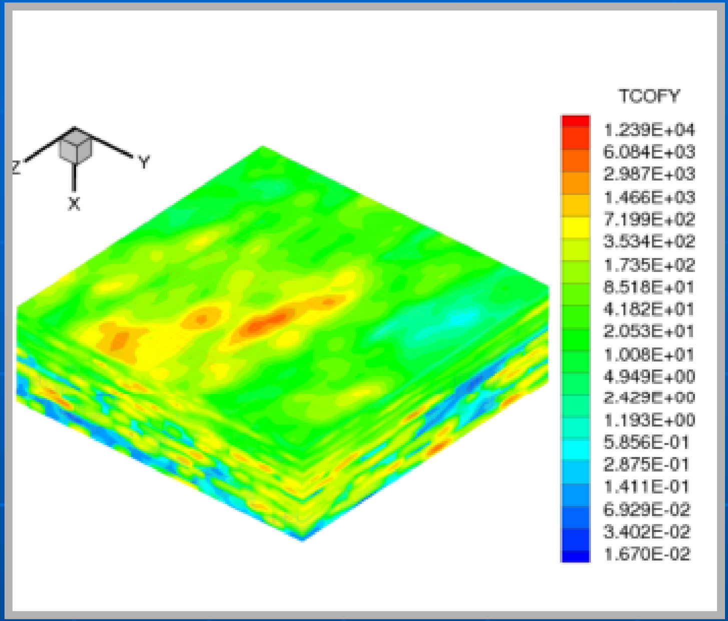

Oil pressure and water saturation @ 3 yrs

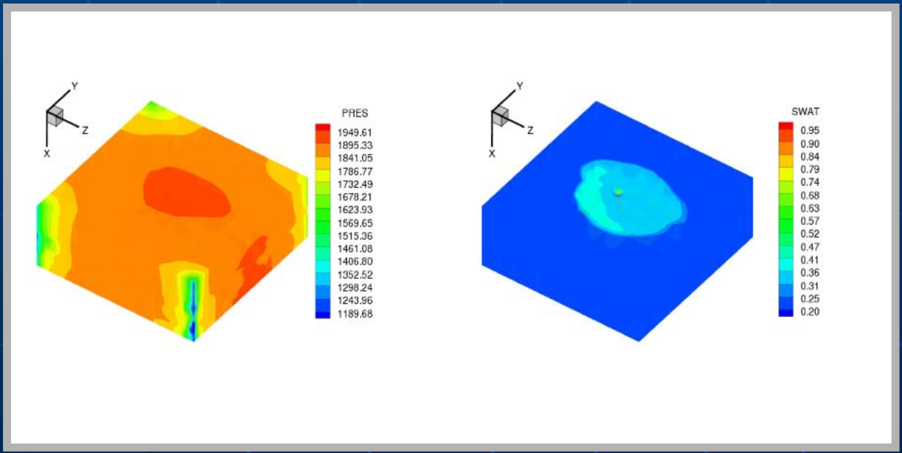

Gas saturation and propane conc. @ 3 yrs

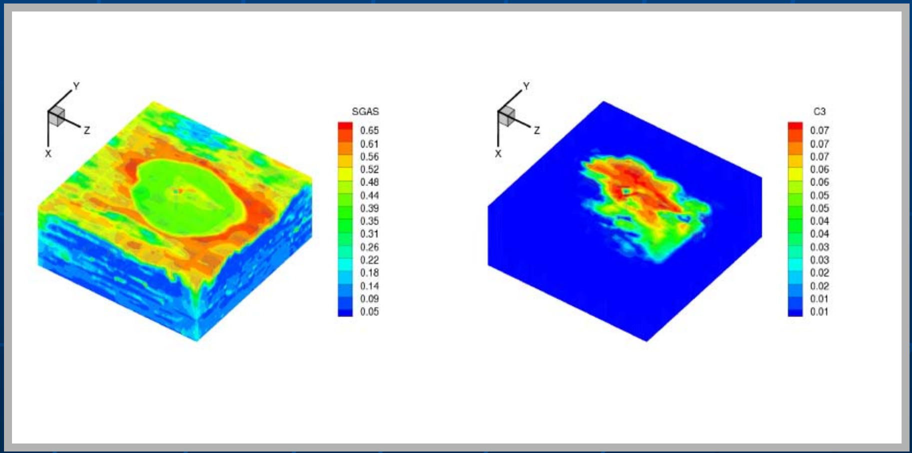

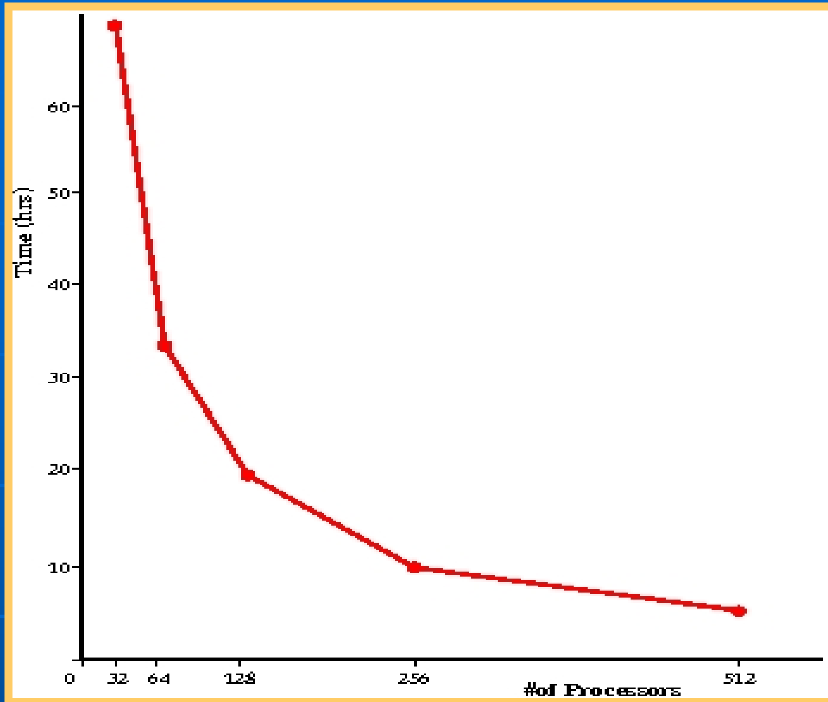

Parallel Scalability

Texas Advanced Computing Center
The University of Texas at Austin

Hardware	
Lonestar: Linux cluster system	Blue GeneP: CNK system, Linux I/O
1,300 Nodes / 5,200 cores	262,144 Nodes / 1,048,576 cores
Processor Arch: 2.66GHz, Dual core, Intel Xeon 5100, Peak: 55 TFlops/s	Processor Arch: 850MHz, IBM CU-08, Peak: ~1 PFlop/s
8 GB/node	2 GB/node
Network: InfiniBand, 1GB/s	Network: 10Gb Eth,1.7GB/s

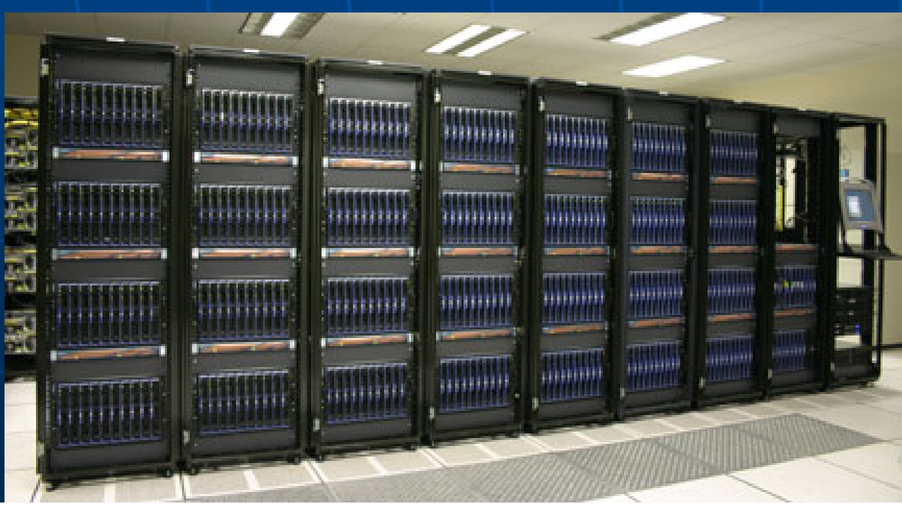

Software
GMRES, BCGS, LSOR, Multigrid.
MPI: MVAPICH2 library for parallel communication

Scalability On Ranger (TACC) & Blue Gene P

GMRES solver with Multigrid Preconditioner
3500ft, 3500 ft, 100ft reservoir
40x160x160=1,024,000 elements
CPUs: 32, 64, 128, 256, 512, 1024

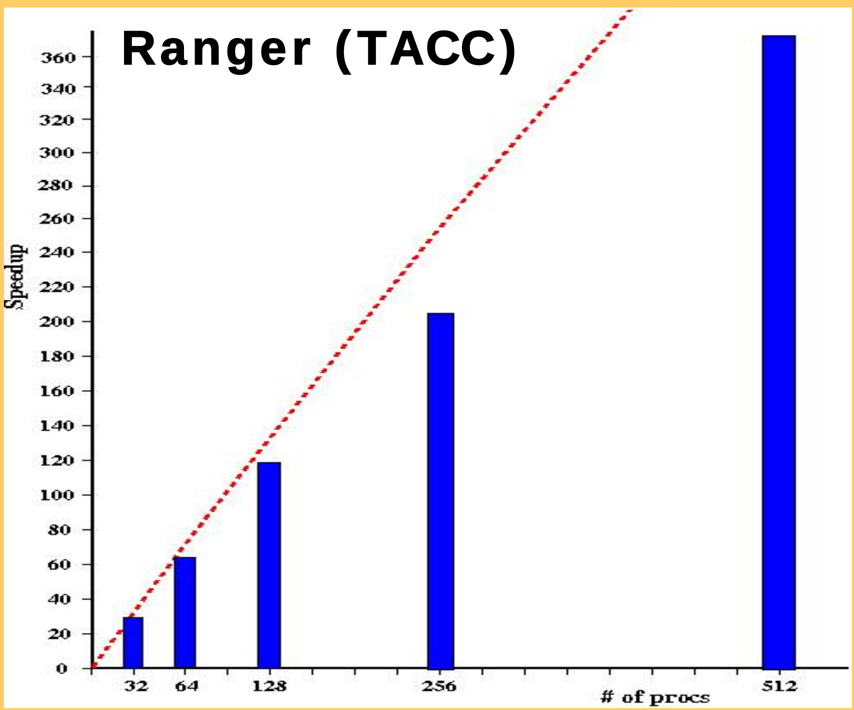

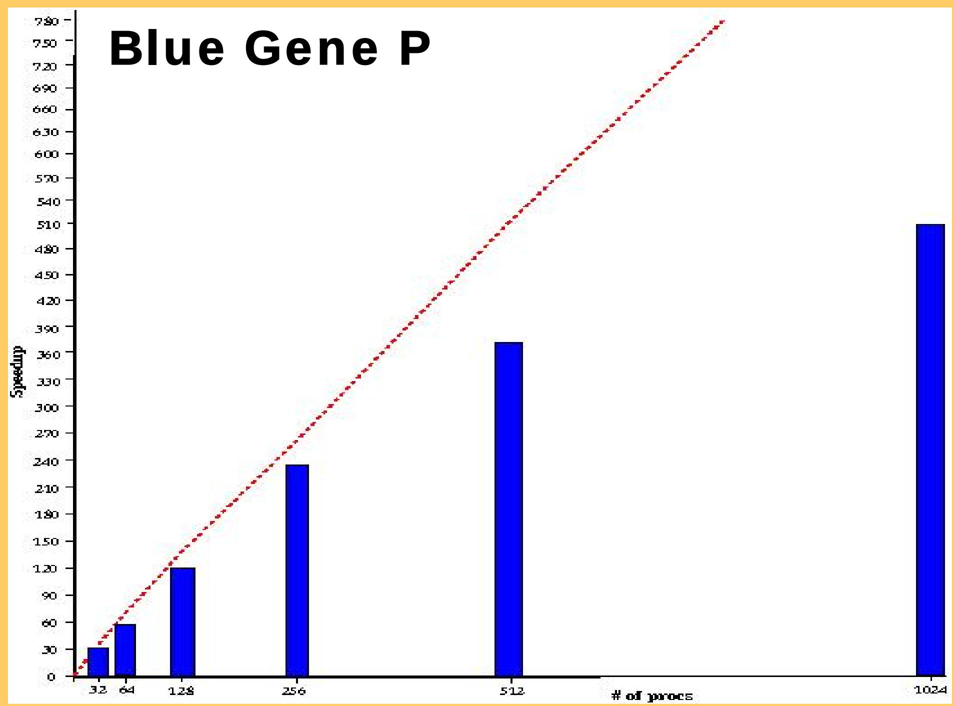

Speedup on Blue Gene (Watson-Shaheen)

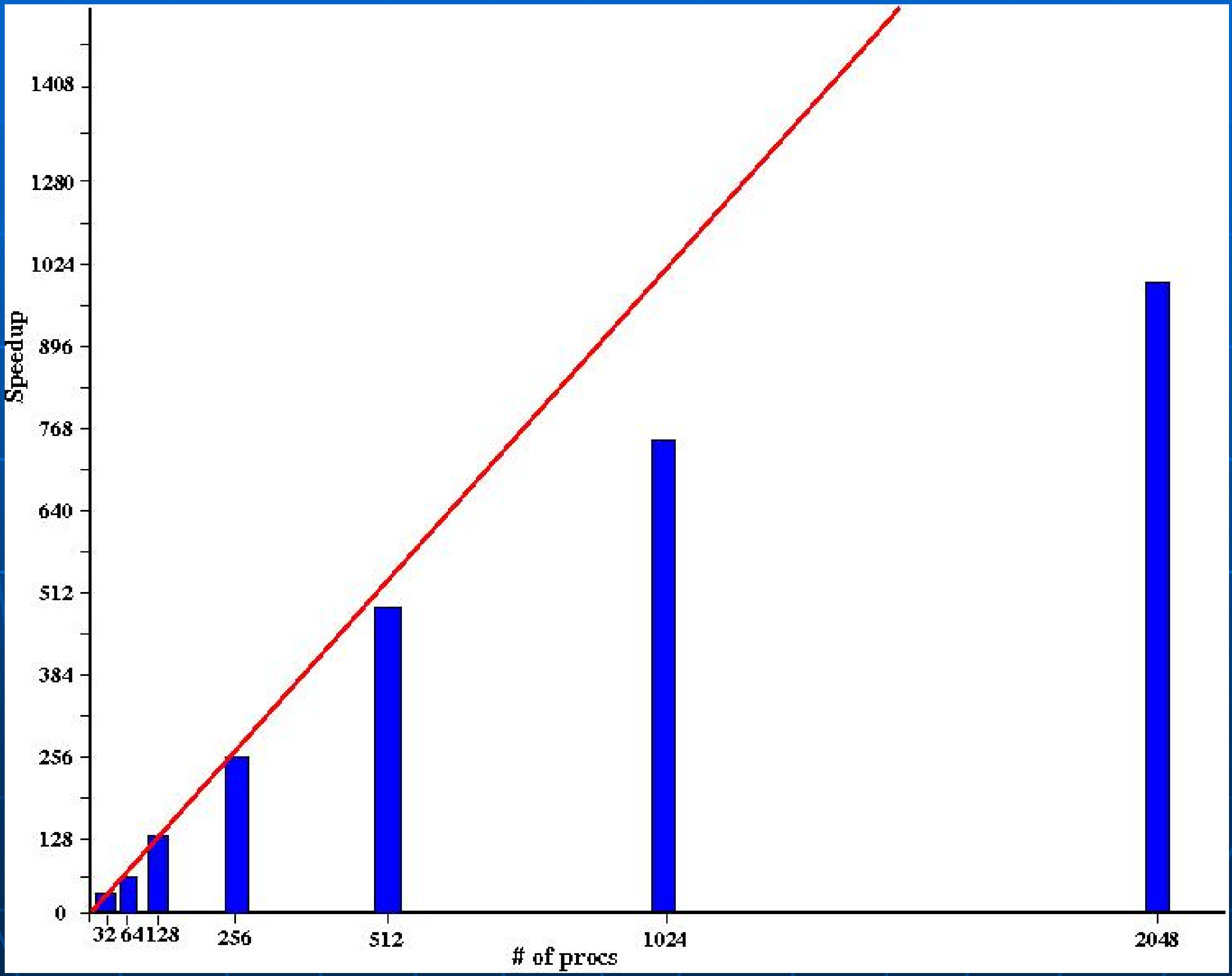

Frio Brine Pilot Site

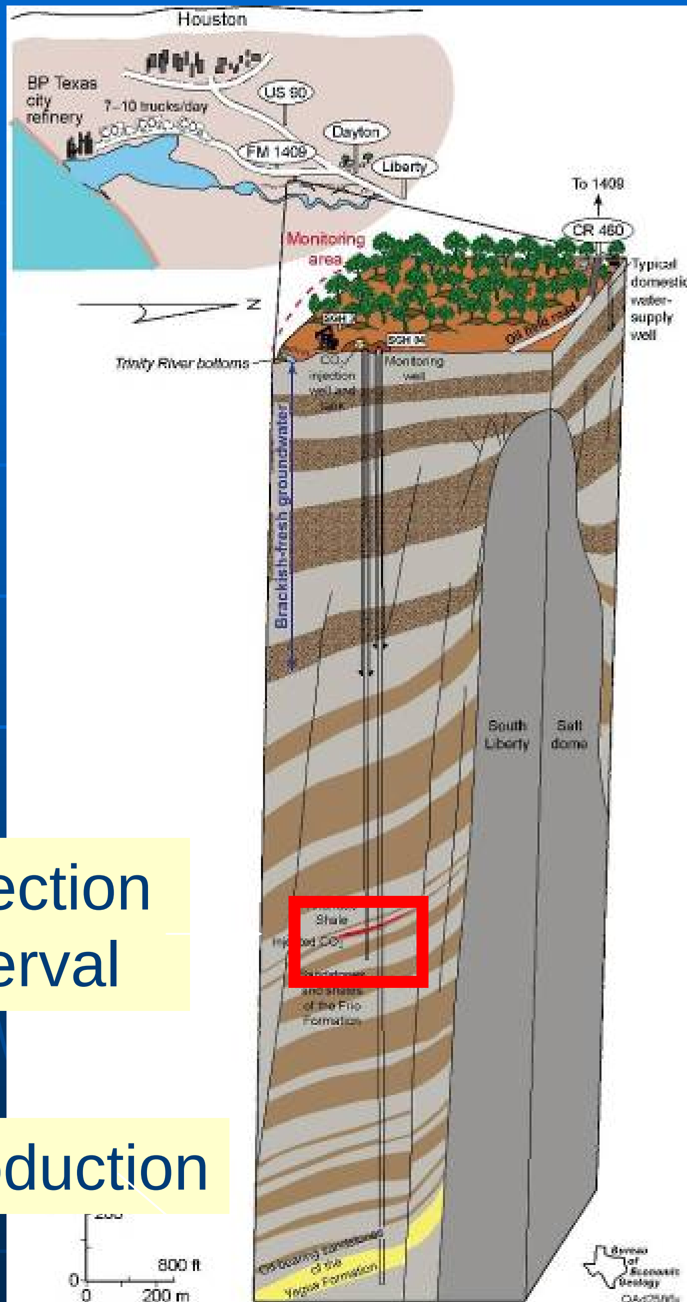

Injection interval

Oil production

- Injection interval: 24-m-thick, mineralogically complex fluvial sandstone, porosity 24%, Permeability 2.5 D
- Unusually homogeneous
- Steeply dipping 16 degrees
- 7m perforated zone
- Seals – numerous thick shales, small fault block
- Depth 1,500 m
- Brine-rock, no hydrocarbons
- 150 bar, 53 C, supercritical CO_2

From Ian Duncan

Frio Modeling using IPARS

Stair stepped approximation on a 50x100x100 grid (~70,000 active elements) has been generated from the given data.

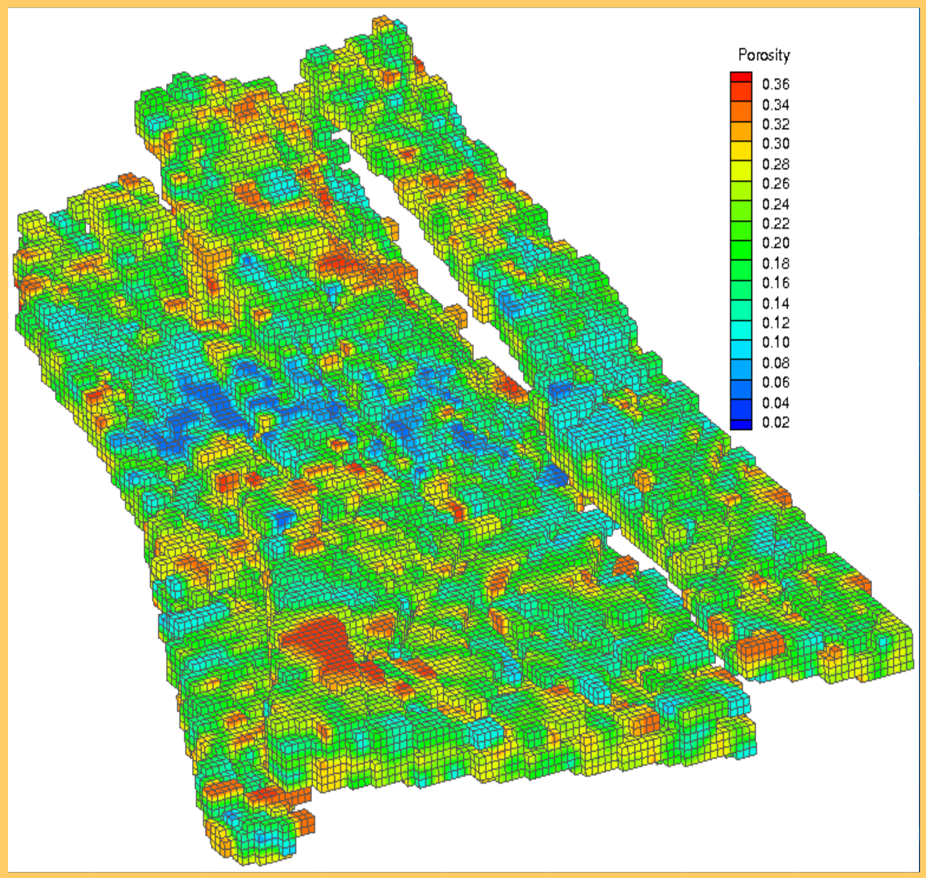

Modeling Temperature for Frio Test

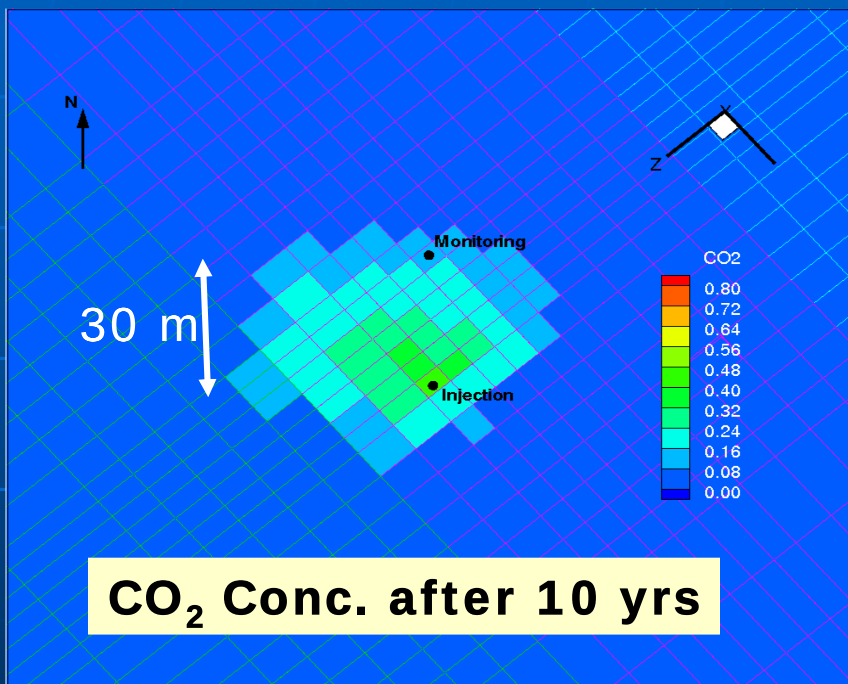

CO_2 Conc. after 10 yrs

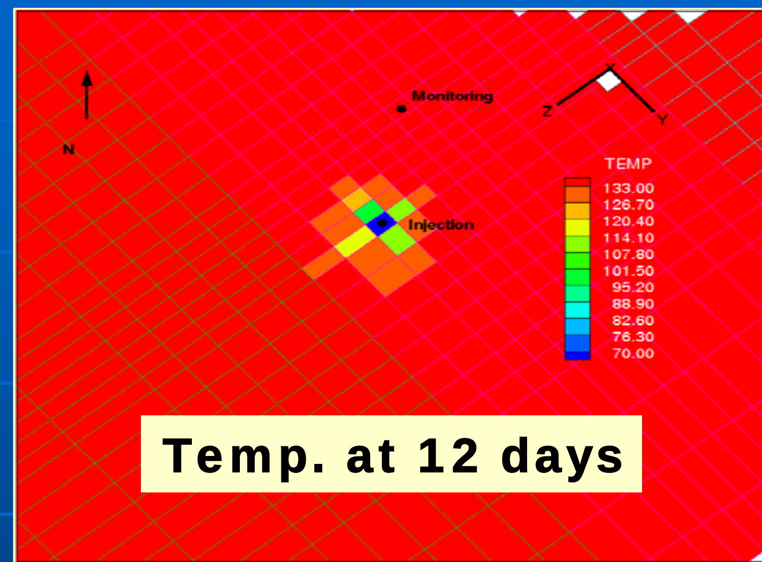

Temp. at 12 days

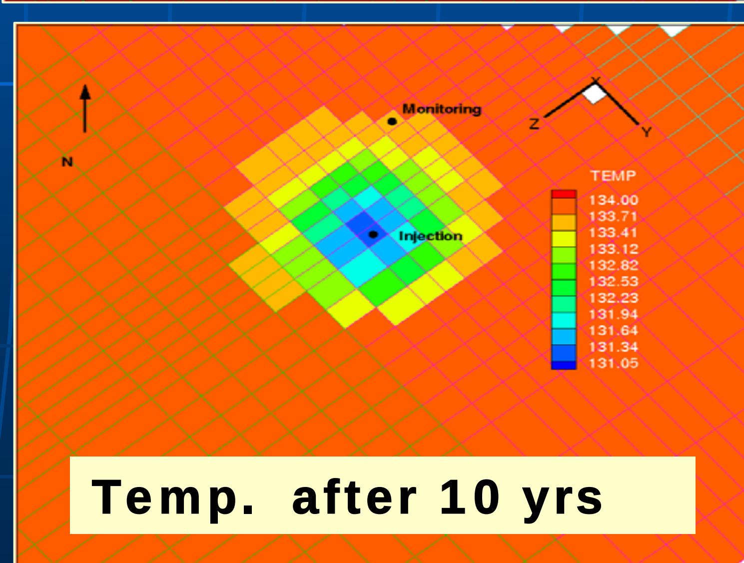

Temp. after 10 yrs

REALISTIC CO2 STUDIES

WAG

HYSTERESIS

CO_2 Injection Scenarios

- Continuous CO_2 injection
- CO_2-Water injection (2:1 Cycle)
- CO_2 injection / Shut in (2:1 cycle)
- One injector at the bottom layer

Inject CO_2 in the bottom 30 ft layer

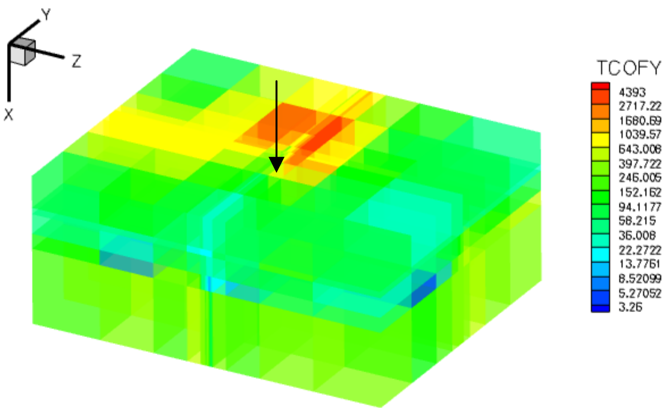

50 x 50 x 5

CO_2 Plume at the end of Injection

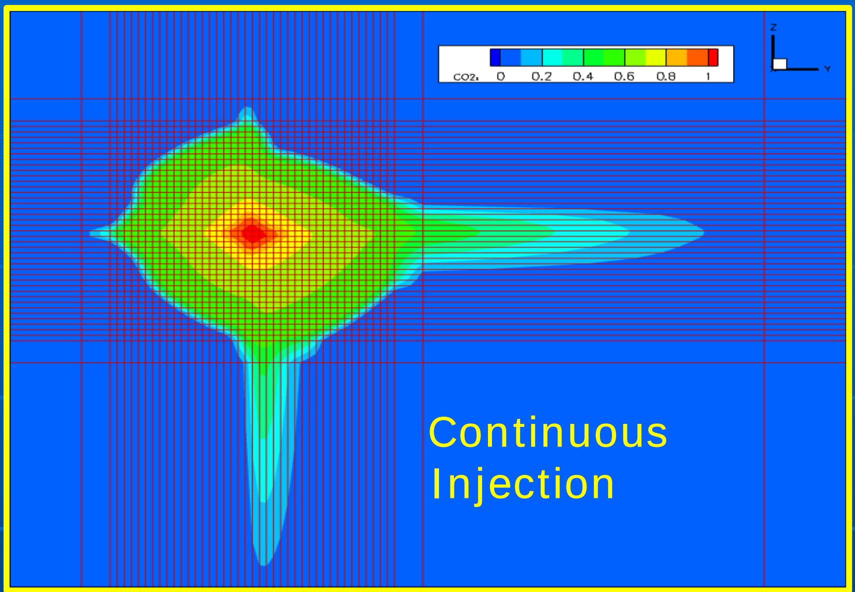

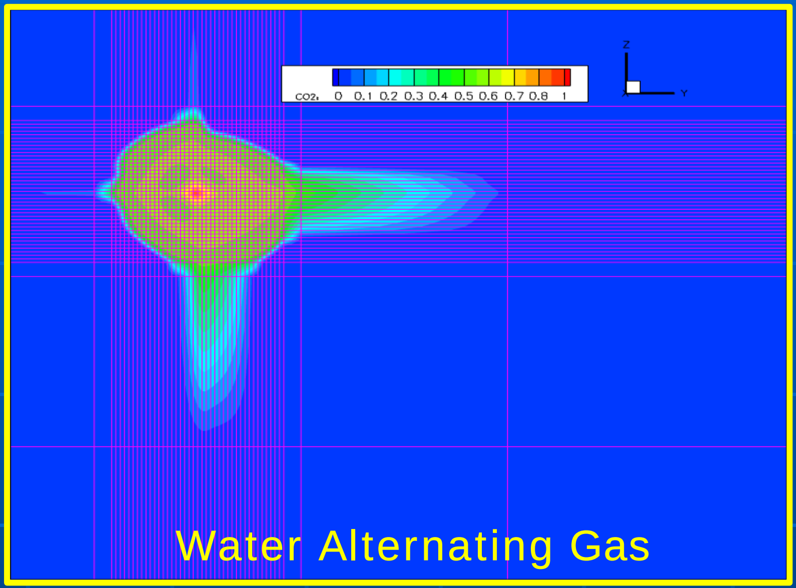

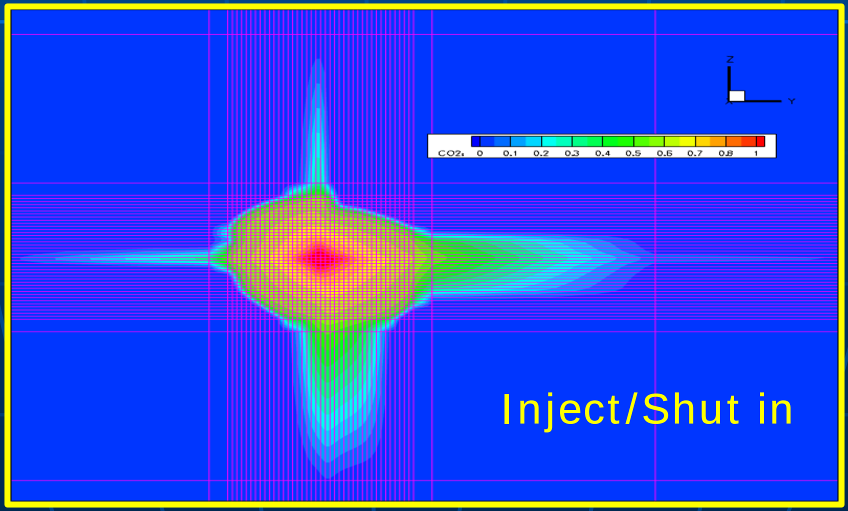

CO_2 plume at the end of Injection (Vertical Profile)

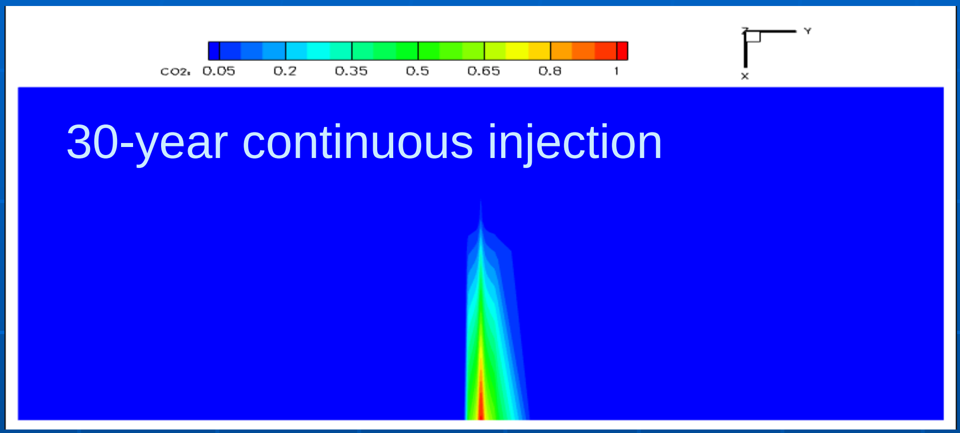

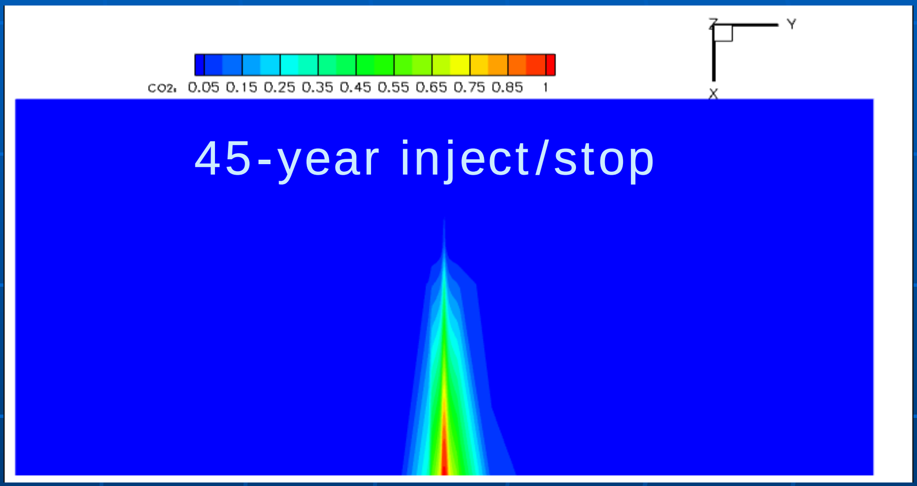

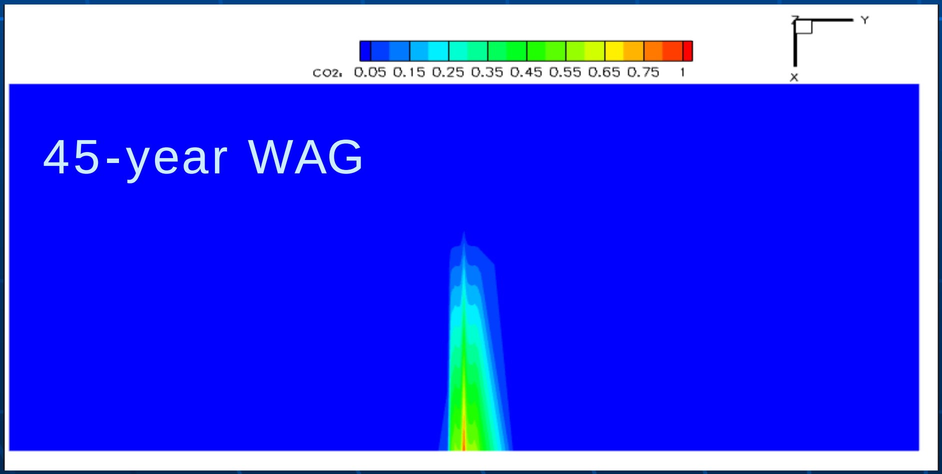

Frio Pilot Test

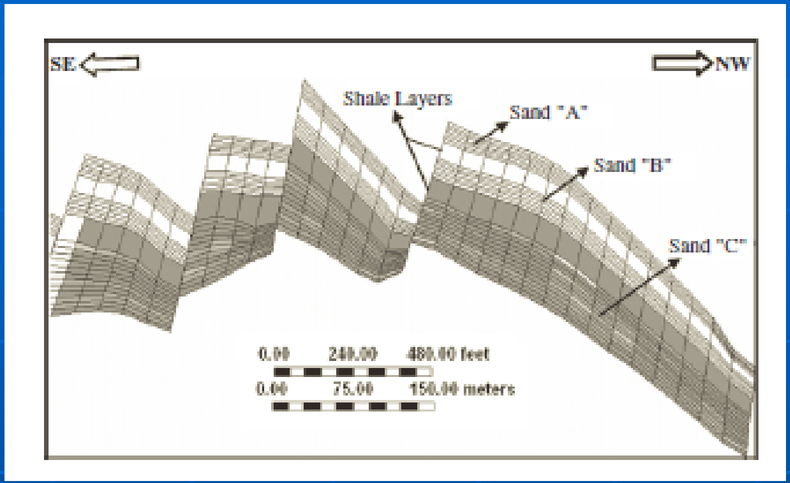

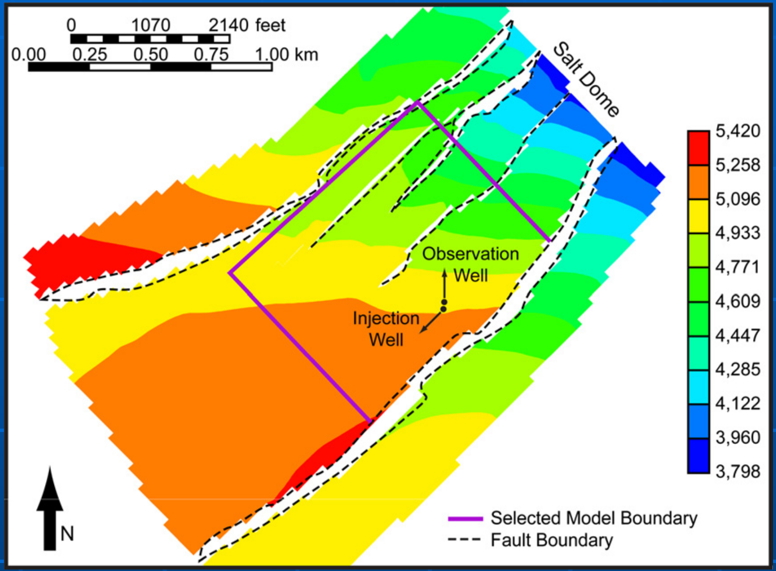

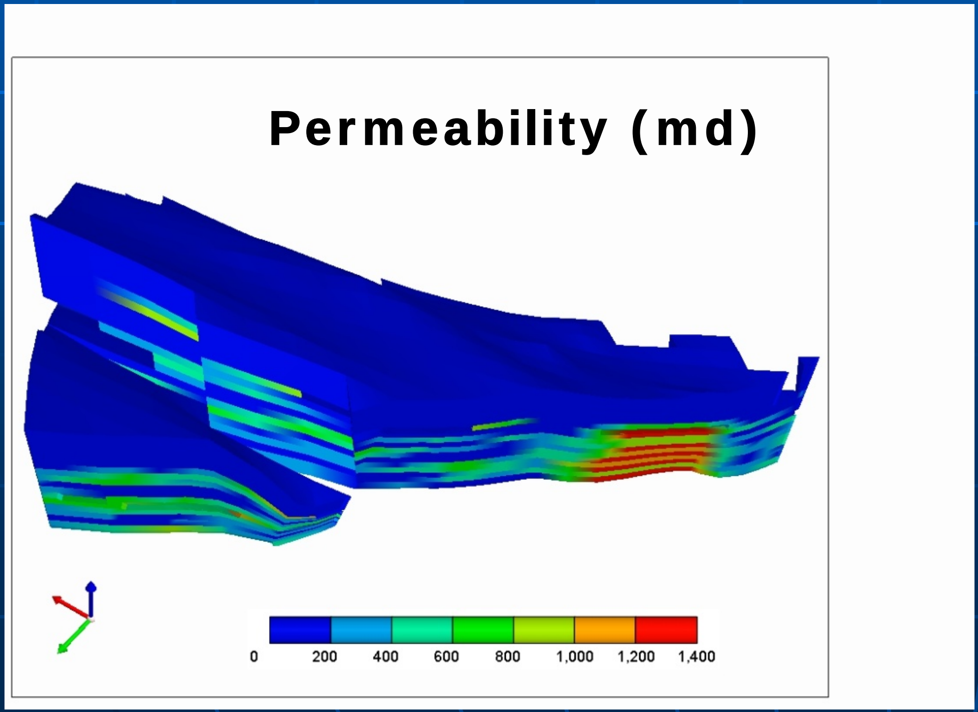

Ghomian et al., 2006

Effect of Gas Relative Permeability – Hysteresis

End of 12 day injection

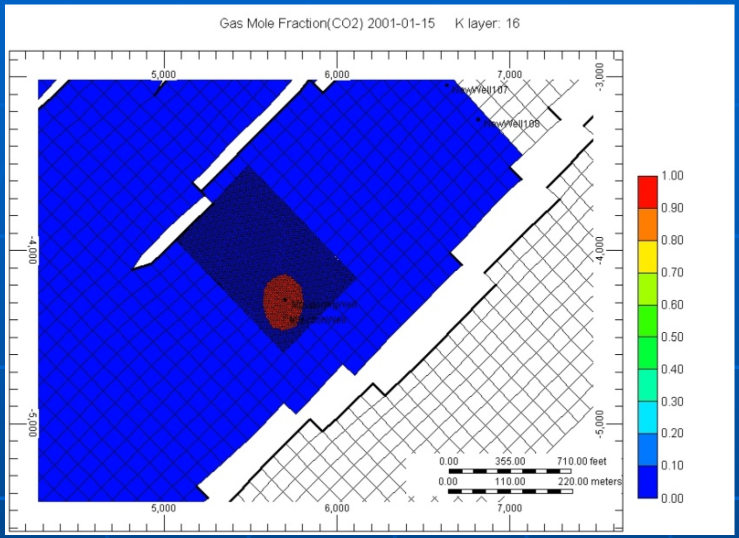

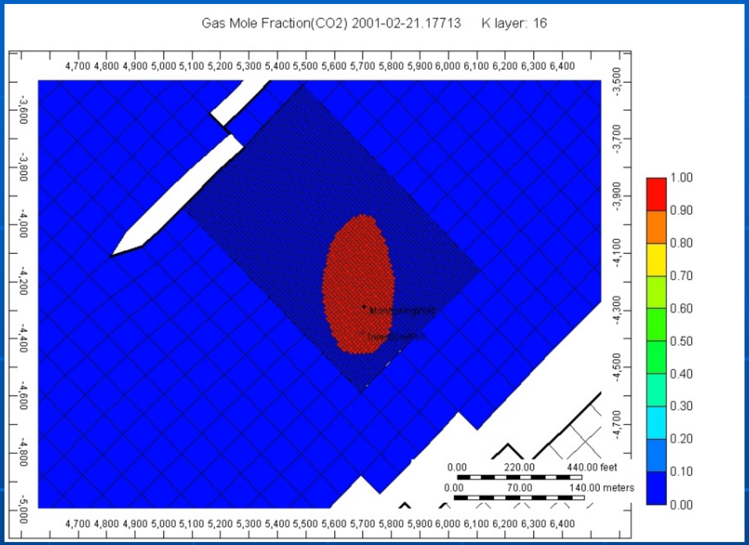

End of 10 yr

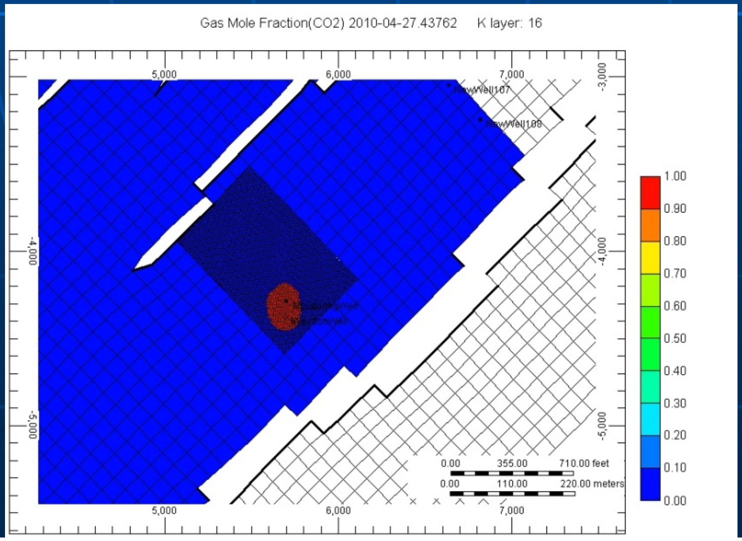

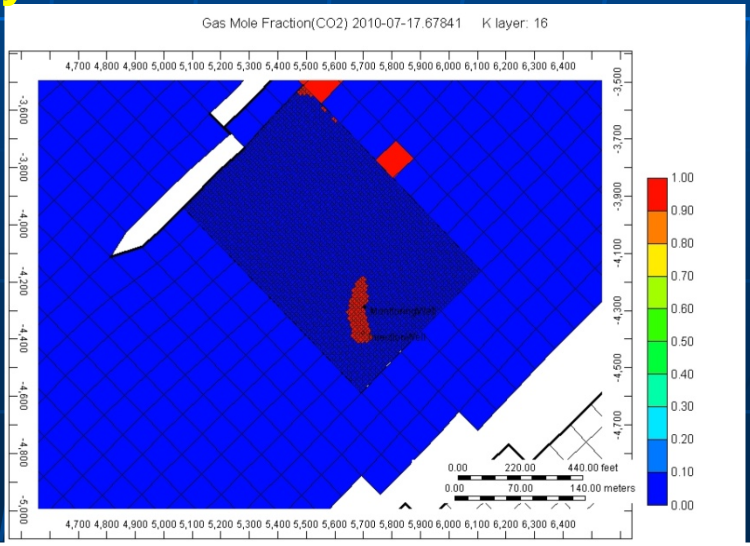

Simulation of Frio Pilot Test

Ghomian et al., 2006

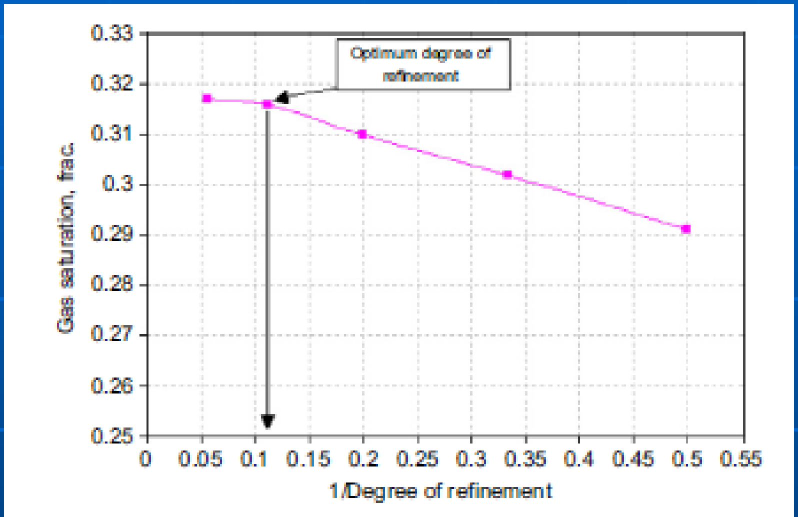

- ✓ 1500 m deep, 6 m thick
- ✓ 30 m inj – monitoring wells
- ✓ T = 57 C
- ✓ 5- 25 dip angle
- ✓ K = f (ϕ)
- ✓ S_{wir} and s_{gr} = f (k, ϕ)

At 10 yrs:
55% as residual CO_2
45% dissolved in brine

83 x 62 x 26 (212,366 cells)
10' x 10' x 2.5' local mesh refinement
No temperature modeling
No geomechanics
No geochemistry
1 – 3 hrs cpu per run

On Prediction of Realistic CO_2 Tests

- Fluid properties as a function of pressure, temperature, composition
  - Viscosity, density, interfacial tension, phase behavior
- Rock dependent relative permeability and capillary pressure as a function of
  - Saturation, composition, saturation history (hysteresis), IFT
- Rock reaction to pressure changes and subsequent impact on pore volumes and permeability (geomechanics)
- Reactions of rock minerals and injected CO2 (geochemistry)
- Model estimators that include upscaling and downscaling for property manipulations for coarse/fine grid
- Upscale strategy for CO_2 storage (if needed)
- Increase grid resolution to improve the quality of model results
  - Increase CPU and memory requirements
  - Faster numerical methods – dynamic grid refinement based on a posteriori error estimators that include upscaling and down scaling, efficient solvers
  - Efficient parallelization methods
  - Optimization and Uncertainty analysis

Computational Components

- High Fidelity Algorithms for Treating Relevant Physics -- Complex Nonlinear Systems (coupled near hyperbolic & parabolic/ elliptic systems with possible discrete models)
  - Locally Conservative Discretizations (mixed fem, control volume and/or discontinuous Galerkin)
- Multiscale (spatial & temporal multiple scales)
- Multiphysics (Darcy flow, biogeochemistry, thermal, geomechanics)
- Robust Efficient Physics-based Solvers (ESSENTIAL)
- A Posteriori Error Estimators

- Decision Theory: Closed Loop Optimization
- Parameter Estimation (history matching) and Uncertainty Quantification (Impt. monitoring leakage)

- Computationally intense:
- Distributed Computing
- Dynamic Steering

Motivation

- Both DG and MFE are locally mass-conservative
- Real world heterogeneities such as thin faults, fractures and pinchouts, internal boundaries, geological layers can be computationally expensive
- Multiphysics applications necessitate coupling of DG and Mixed FEM
- Local mesh refinement

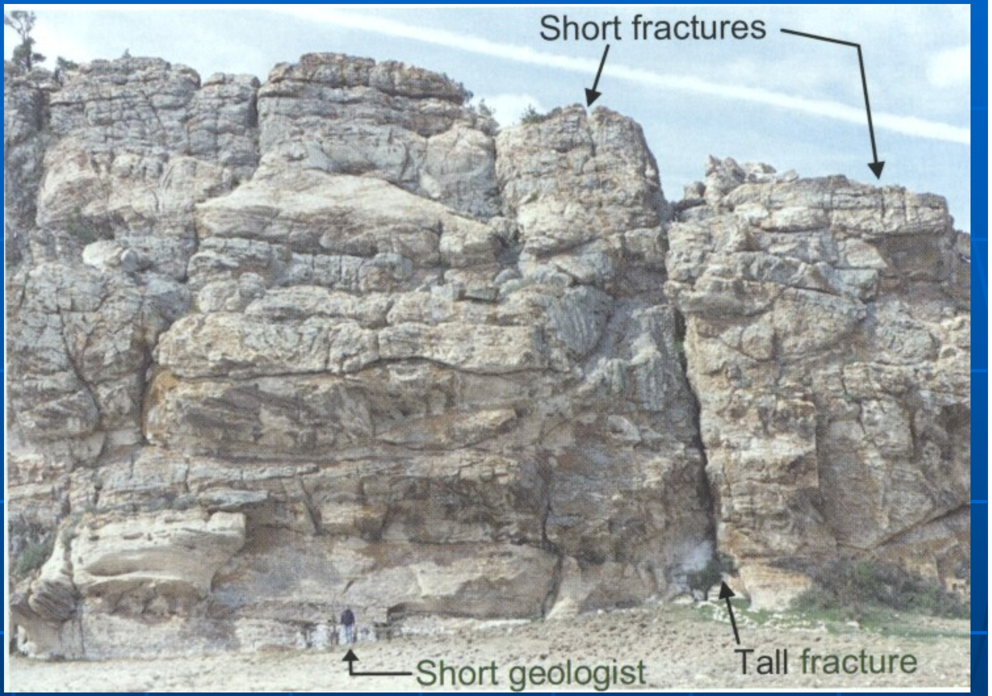

Eolian sandstone of the Weber Formation, Whiskey Gap, Wyoming

(photo taken from Wayne Narr, David W. Schechter, and Laird B. Thompson. Naturally Fractured Reservoir Characterization. Society of Petroleum Engineers, 2006.)

Solution

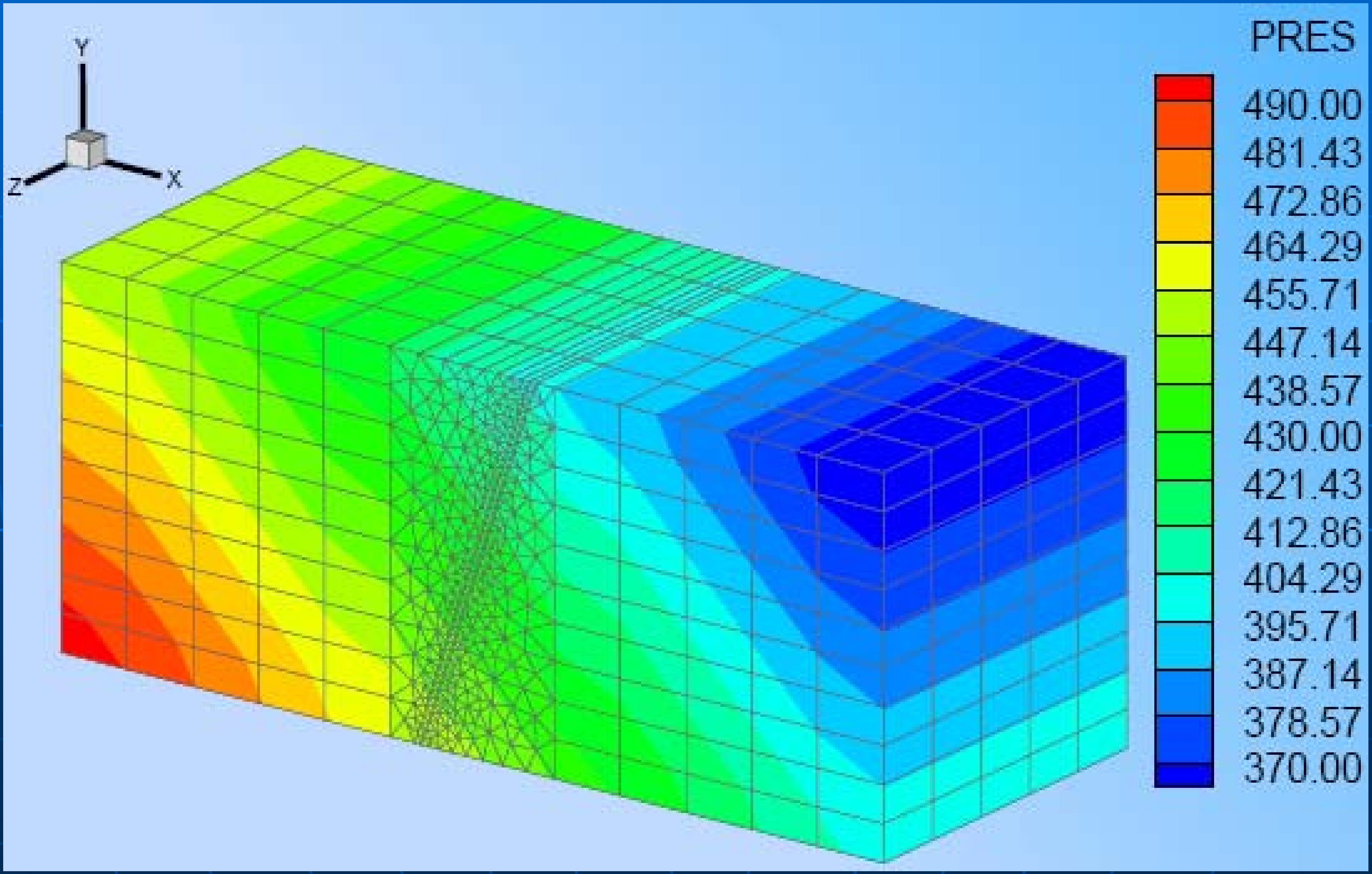

Y
Z
X
PRES
490.00
481.43
472.86
464.29
455.71
447.14
438.57
430.00
421.43
412.86
404.29
395.71
387.14
378.57
370.00

Why Multiscale?

- Subsurface properties vary on the scale of millimeters
- Computational grids can be refined to the scale of meters or kilometers
- Multiscale methods are designed to allow fine scale features to impact a coarse scale solution
  - Variational multiscale finite elements
    - Hughes et al 1998
    - Hou, Wu 1997
    - Efendiev, Hou, Ginting et al 2004
  - Mixed multiscale finite elements
    - Arbogast 2002
    - Aarnes 2004
  - Mortar multiscale finite elements
    - Arbogast, Pencheva, Wheeler, Yotov 2004
    - Yotov, Ganis 2008

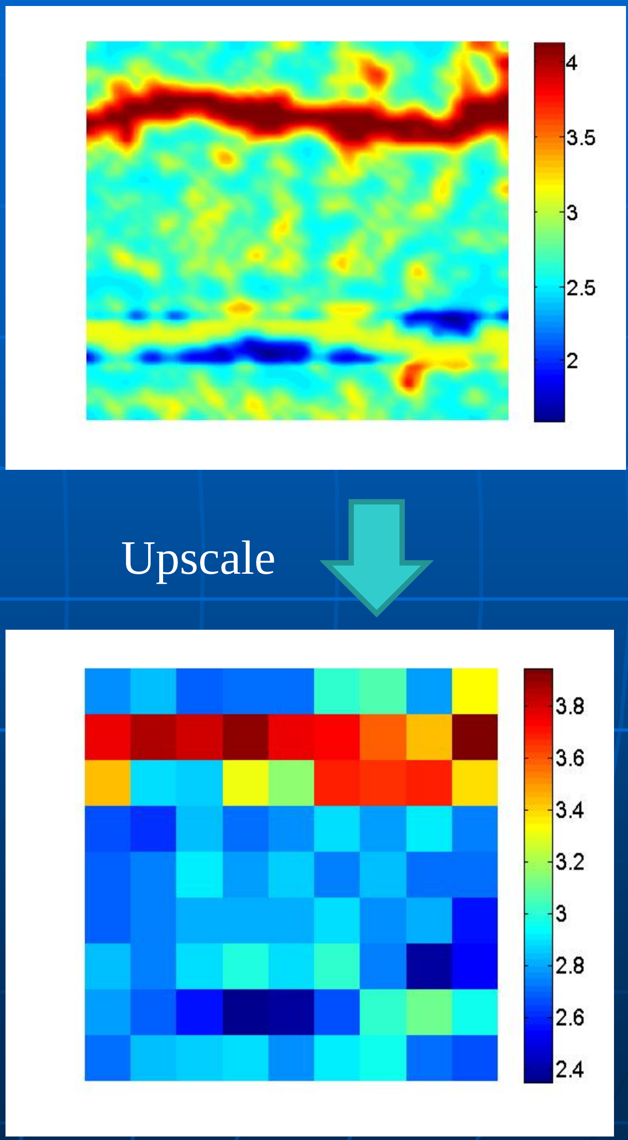

Basic Idea of the Multiscale Mixed Mortar Method

1. **Localization.** Divide Ω into many small subdomains (or coarse elements of scale H), over which the original PDE is imposed.
2. **Fine-scale effects.** The subdomains are given Dirichlet boundary conditions $p = \lambda$ on Γ and solved on the fine scale h to define the local solution.
3. **Global coarse-grid problem.** The weakly defined flux mismatch (jump in $\mathbf{u} \cdot \nu$) on Γ is used to define a better λ on scale $H > h$, and we iterate the previous step until convergence is attained.
4. **Fine-grid (re)construction.** We obtain a fully resolved and fully coupled approximate solution if λ is approximated in a higher order space.

By using a higher order mortar approximation, we compensate for the coarseness of the grid and maintain good (fine scale) overall accuracy.

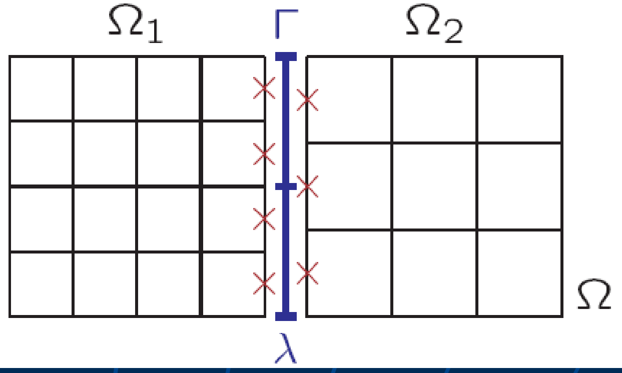

Multiscale Mortar Mixed Finite Element Method

Key idea. On the interface

- Use only a few degrees of freedom (manage the linear algebra).
- Use higher order approximation (maintain accuracy).

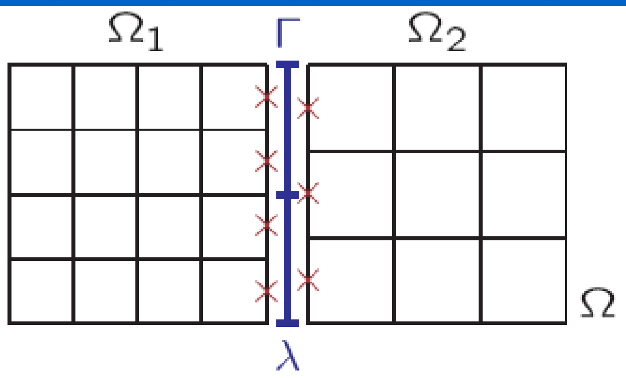

Finite element spaces.

- **Subdomain.** $\mathbf{V}_{h,i} \times W_{h,i}$ is usual mixed space with polynomials of degree $k-1$ on mesh of spacing $h > 0$ on Ω_i.
- **Mortar.** $M_{H,ij}$ is continuous or discontinuous polynomials of degree $m-1$ on mesh of spacing $H > h$ on Γ_{ij}.

Mortar method. Find $\mathbf{u}_h \in \mathbf{V}_h$, $p_h \in W_h$, $\lambda_H \in M_H$ such that

$$\begin{cases} (K^{-1}\mathbf{u}_h, \mathbf{v})_{\Omega_i} = (p_h, \nabla \cdot \mathbf{v})_{\Omega_i} - \langle \lambda_H, \mathbf{v} \cdot \nu_i \rangle_{\Gamma_i} & \forall \mathbf{v} \in \mathbf{V}_{h,i} \\ (\nabla \cdot \mathbf{u}_h, w)_{\Omega_i} = (f, w)_{\Omega_i} & \forall w \in W_{h,i} \\ \sum_i \langle \mathbf{u}_h \cdot \nu_i, \mu \rangle_{\Gamma_i} = 0 & \forall \mu \in M_H \end{cases}$$

Remark. The last equation enforces weak continuity of flux on Γ.

Construction of a Multiscale Basis

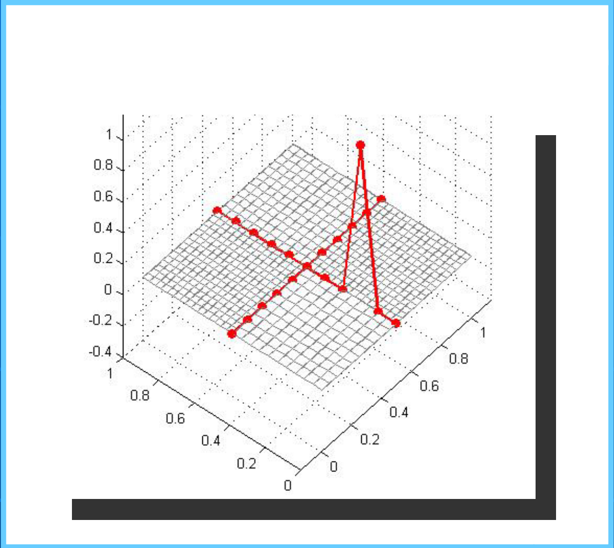

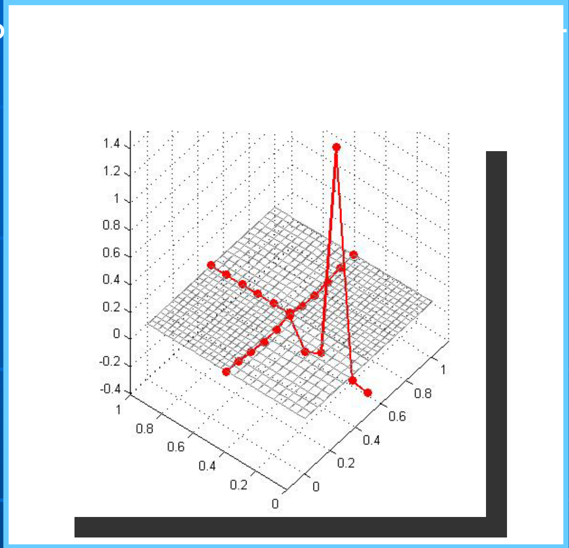

$$\begin{cases} (K^{-1}\boldsymbol{u}^*(\lambda_j), \boldsymbol{v})_{\Omega_i} &= (p^*(\lambda_j), \nabla \cdot \boldsymbol{v})_{\Omega_i} - \langle \lambda_j, \boldsymbol{v} \cdot \nu_i \rangle_{\Gamma_i}, \\ (\nabla \cdot \boldsymbol{u}^*(\lambda_j), w)_{\Omega_i} &= 0. \end{cases}$$

Domain Decomposition and Multiscale

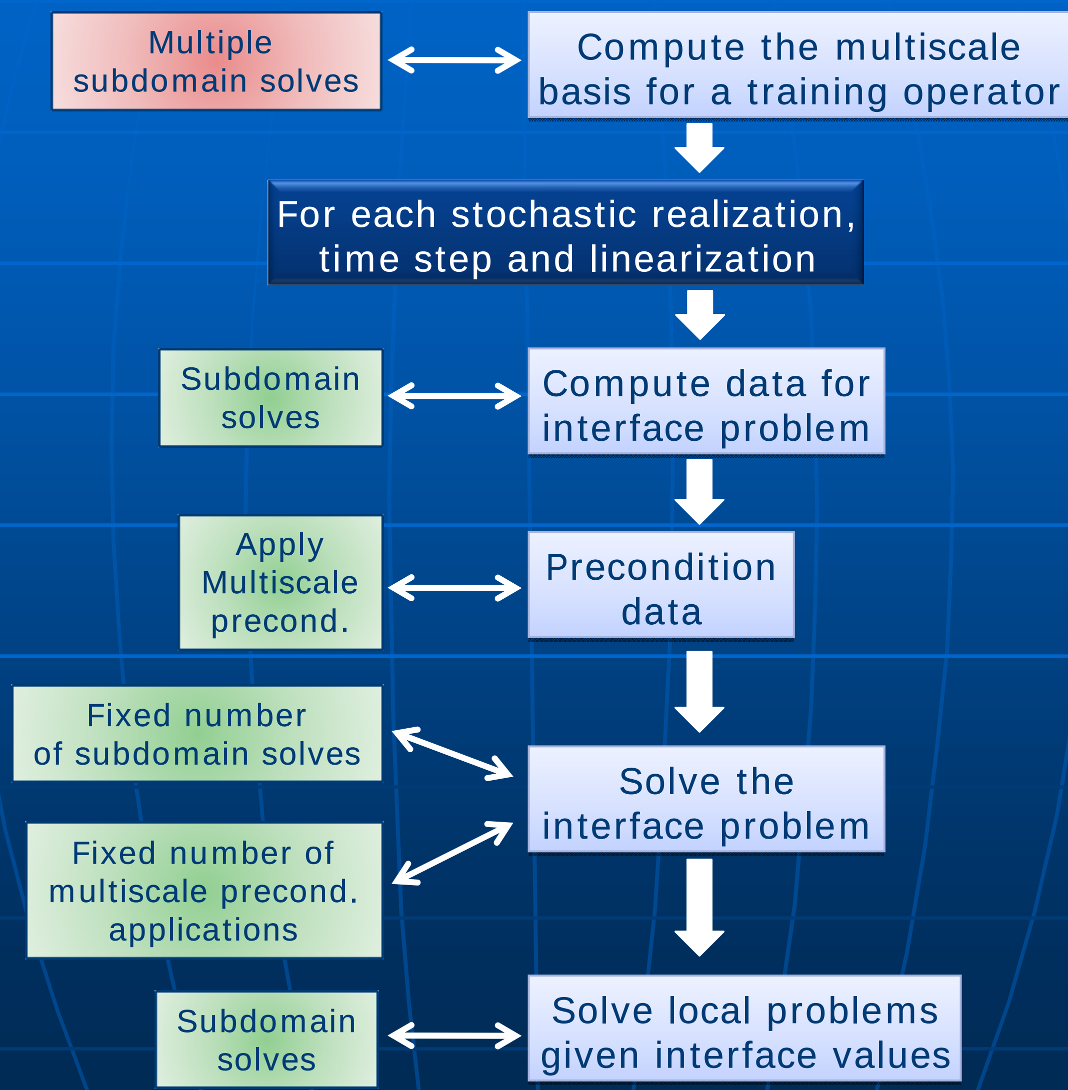

Example: Uncertainty Quantification

- 360x360 grid
- 25 subdomains of equal size
- 129,600 degrees of freedom
- Continuous quadratic mortars
- Karhunen-Loéve expansion of the permeability truncated at 9 terms
- Second order stochastic collocation
- 512 realizations
- Training operator based on mean permeability

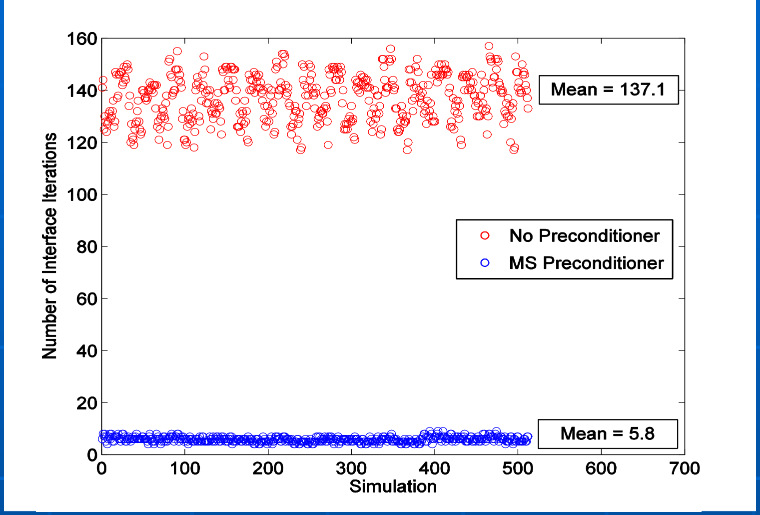

Mean Permeability
Number of Interface Iterations

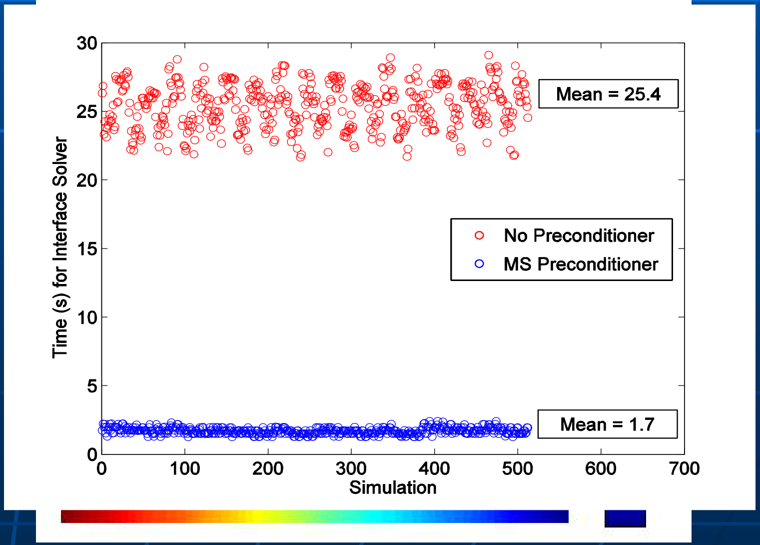

Interface Solver Time
Mean Pressure

Example: IMPES for Two Phase Flow

- 360x360 grid
- 25 subdomains of equal size
- 129,600 degrees of freedom
- Continuous quadratic mortars
- 50 implicit pressure solves
- 100 explicit saturation time steps per pressure solve
- Training operator based on initial saturation

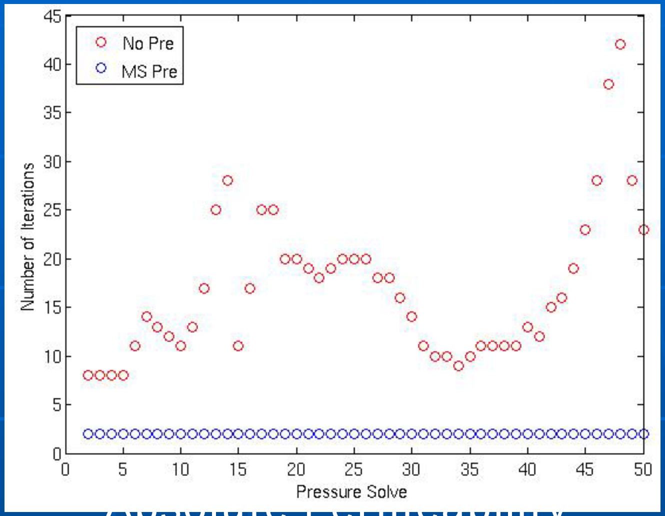

Absolute Permeability
Number of Interface Iterations

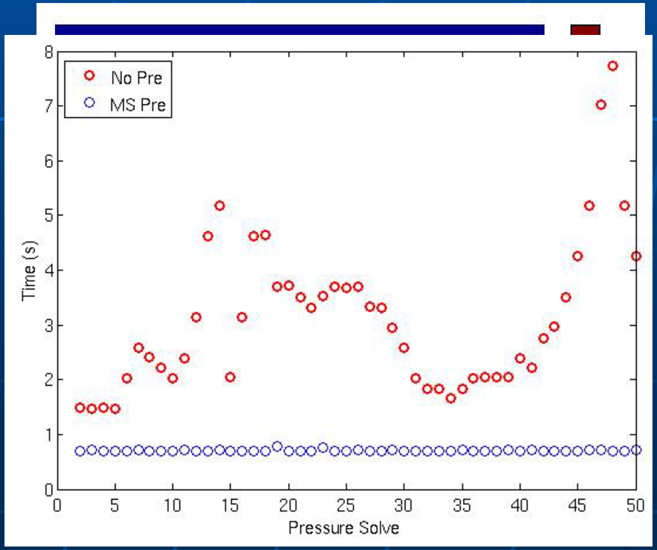

Initial Saturation
Interface Solver Time

Multipoint Flux Mixed Finite Element

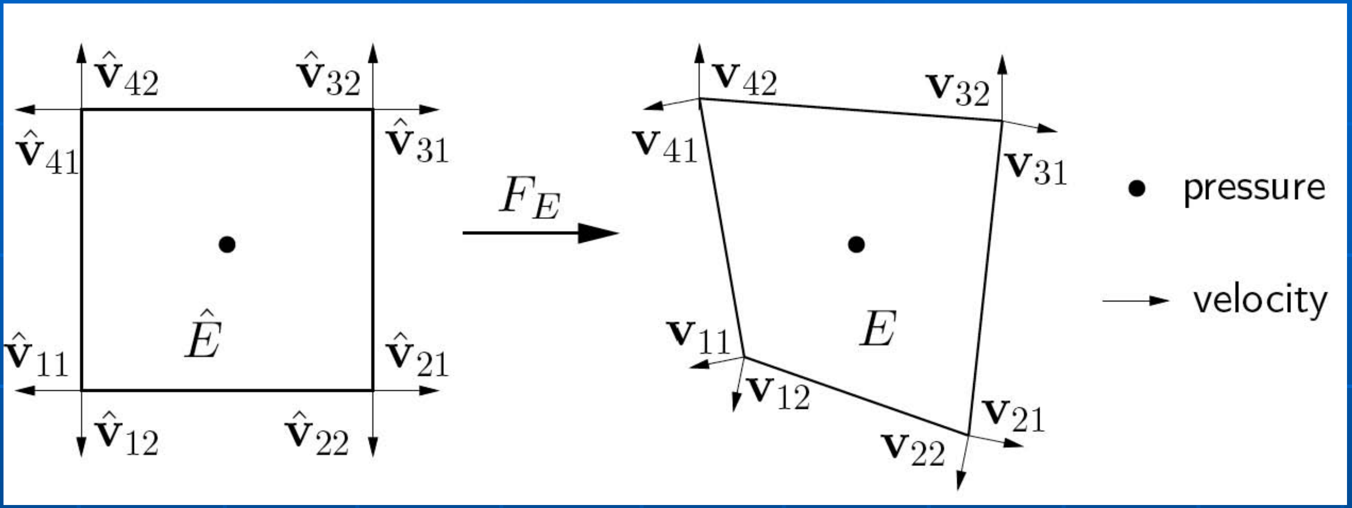

$$(DF_E)_{ij} = \frac{\partial F_i}{\partial \hat{x}_j}$$

$$J_E = |\det(DF_E)|$$

BDM1 Space on reference element:

$$\hat{V}(\hat{E}) = \begin{pmatrix} \alpha_1 \hat{x} + \beta_1 \hat{y} + \gamma_1 + r\hat{x}^2 + 2s\hat{x}\hat{y} \\ \alpha_2 \hat{x} + \beta_2 \hat{y} + \gamma_2 - 2r\hat{x}\hat{y} - s\hat{y}^2 \end{pmatrix}$$

$$V_h(E) = \frac{1}{J_E} DF_E \hat{V}(\hat{E}) \circ F_E^{-1}$$

$$W_h(E) = const$$

MFMFE on Quadrilaterals and Hexahedra

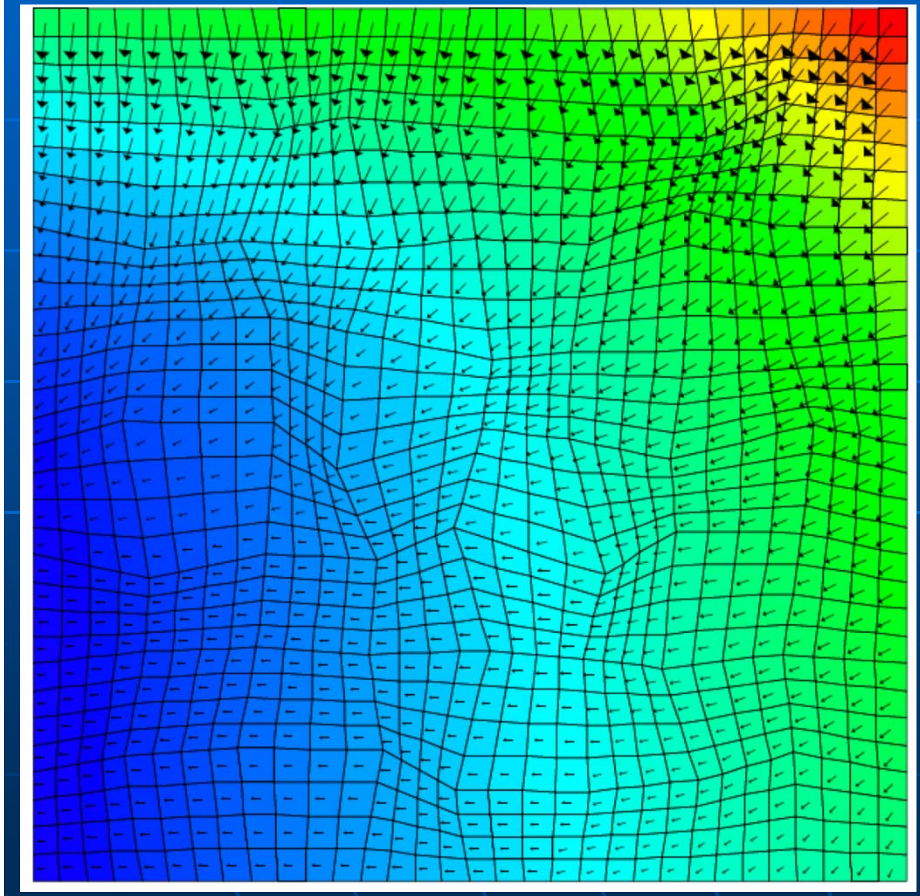

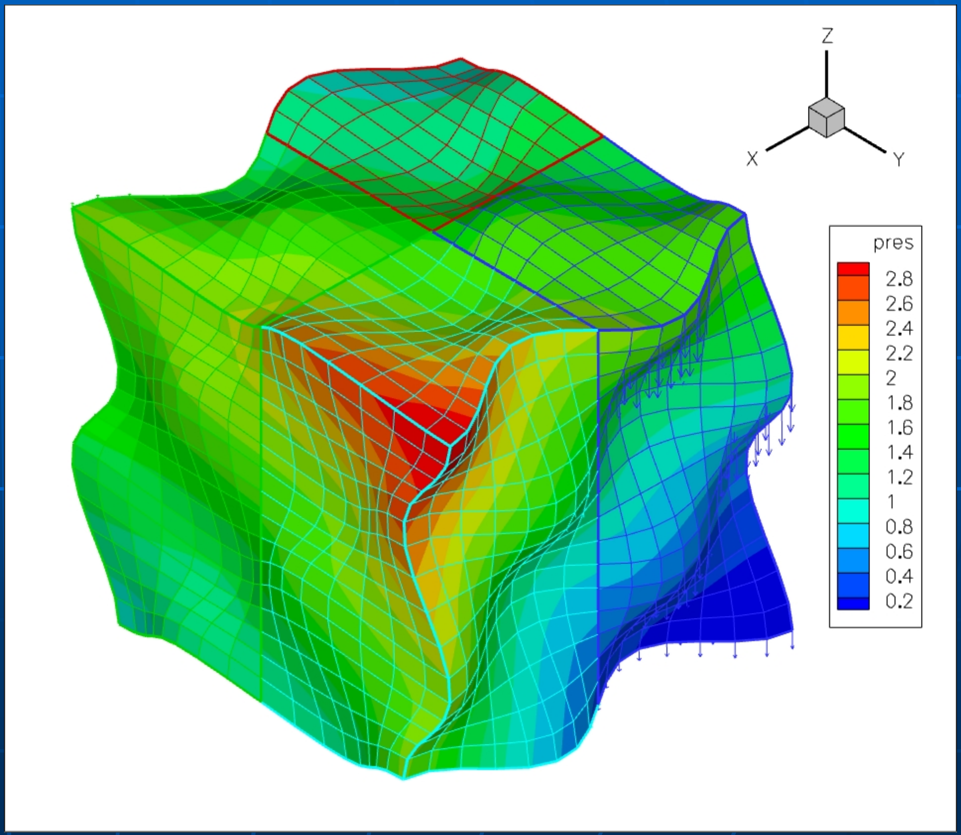

Convergence of MFMFE

Find $u_h \in V_h$ and $p_h \in W_h$

$$(K^{-1}u_h, v)_Q = (p_h, \nabla \cdot v), \qquad v \in V_h$$
$$(\nabla \cdot u_h, w) = (f, w), \qquad q \in W_h$$

Numerical Quadrature: $(K^{-1}v, q)_{Q,E} = (\kappa^{-1}\hat{q}, \hat{v})_{Q,\hat{E}} \equiv \frac{|\hat{E}|}{4}\sum_{i=1}^{4}\kappa^{-1}(\hat{r}_i)\hat{q}(\hat{r}_i)\cdot \hat{v}(\hat{r}_i)$

$$\kappa = JDF^{-1}\hat{K}(DF^{-1})^T$$

This quadrature rule reduces saddle point problem into cell-centered pressure equation.

Theorem: (Wheeler and Yotov 2005, Ingram and Wheeler and Yotov 2009)
On simplicial and h^2-parallelogram grids, h^2-parallel pipebeds

$$\|u - u_h\|_V + \|p - p_h\|_W \leq Ch$$
$$\|Q_h p - p_h\|_W \leq Ch^2$$

PHYSICS BASED SOLVERS

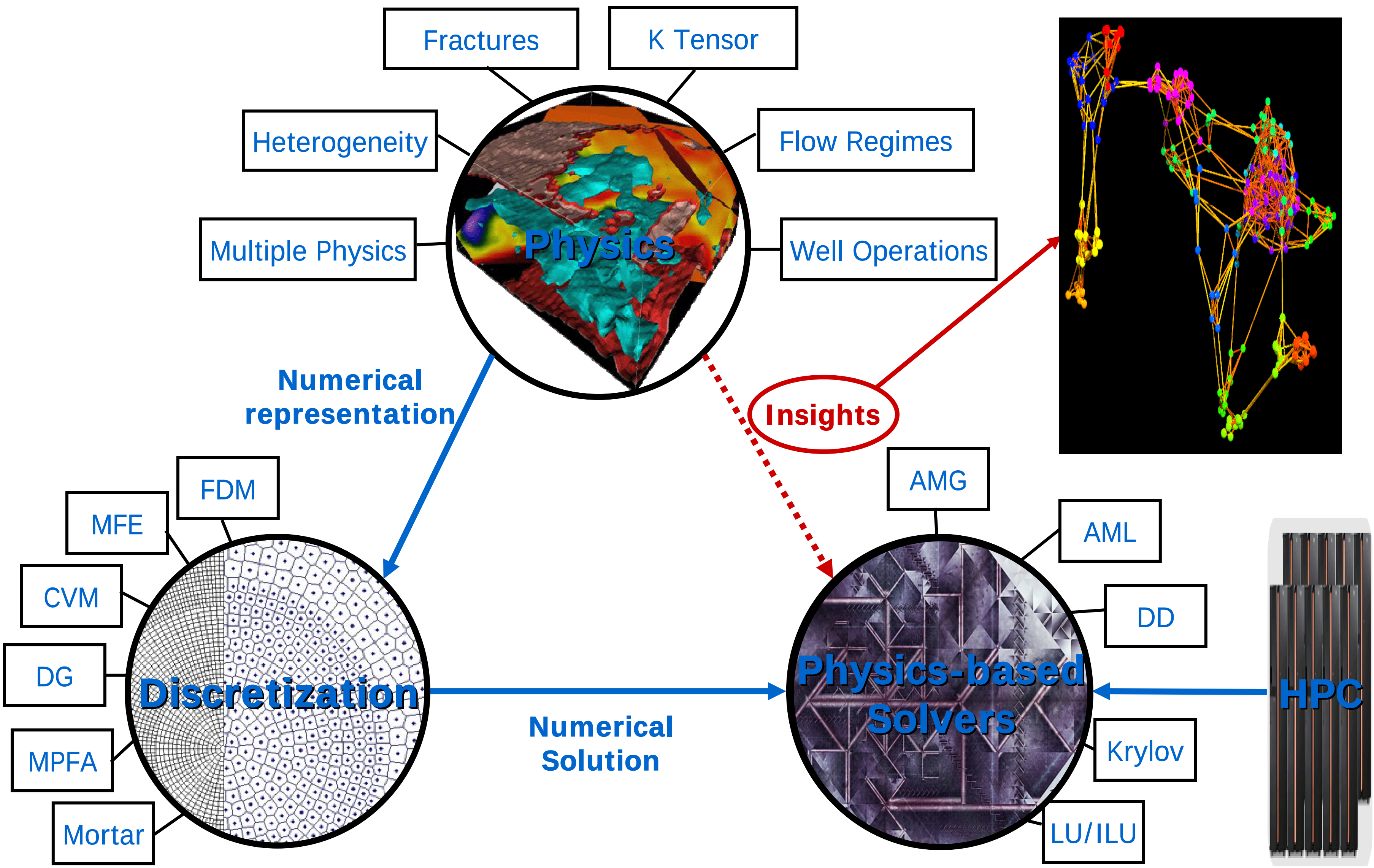

A Posteriori Error Estimates

- Bound computations without knowing the solution:
- Choose norm equivalent to residual
  - Standard for linear problems on conforming spaces (Ainsworth, Babuska, Estep, Johnson, Oden, Rannacher, Verfurth, ...)
  - Extensions to non-conforming and computable bounds (W & Yotov; Arbogast, Pencheva, W & Yotov; Ainsworth; Vohralik; Vohralik & Ern; Pencheva, W, Wildey & Vohralik;
- Estimators need to be
  - Computable
  - Locally efficient for adaptivity
  - Robust (correct and apply to realistic problems, e.g. nonlinear and possibly singular)
  - Incorporate upscaling and downscaling of models ; solver tolerance related to mesh

Ex. – A Highly Oscillating Permeability (Arbogast, Pencheva, W, & Yotov)

Permeability is highly oscillating

$$K = \begin{cases} 105 - 100\sin(20\pi x)\sin(20\pi y), & x, y \in [0, 1/2] \text{ or } x, y \in [1/2, 1], \\ 105 - 100\sin(2\pi x)\sin(2\pi y), & \text{otherwise.} \end{cases}$$

We test AMR with $K = I$.

- 6×6 subdomains.
- Initial subdomain grid 2×2.
- Single mortar element on each interface.

Ex. – A Highly Oscillating Permeability

Magnitude of the velocity after four refinements

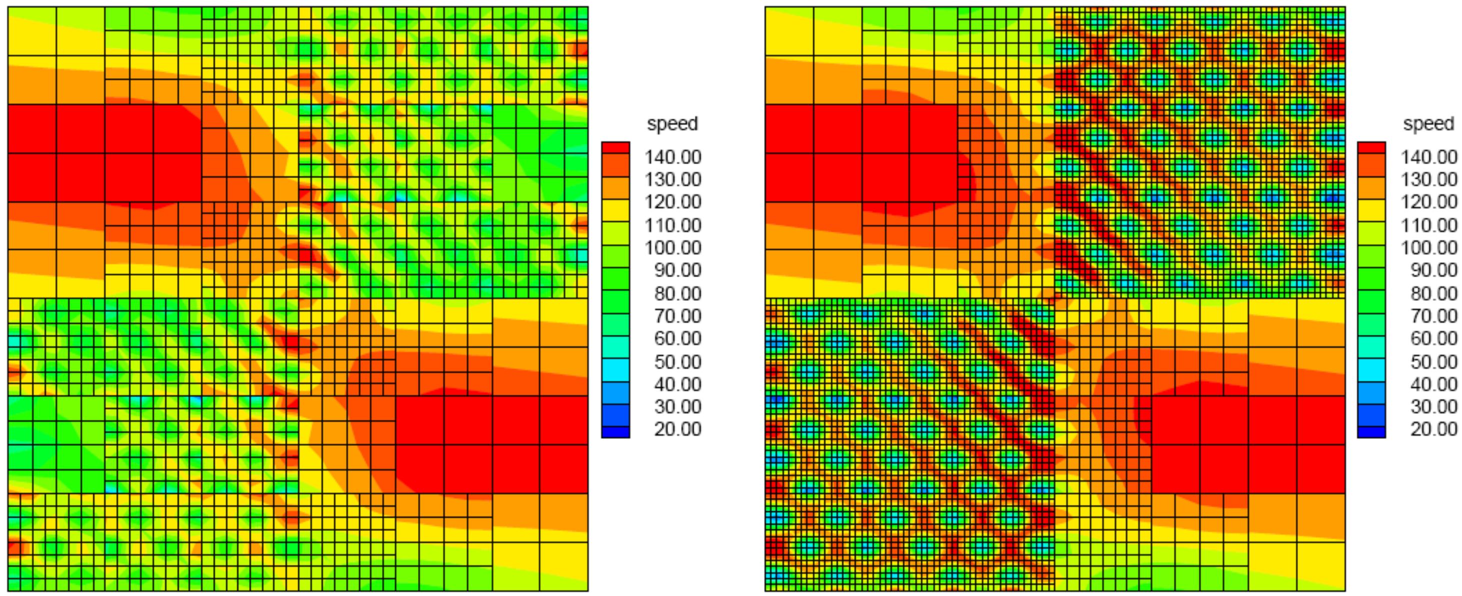

Continuous quadratic mortars — Continuous linear mortars.

Conclusions.

- The highly oscillating velocity is well resolved.
- Refinement along $x = 1/2$ is due to the large jump-flux term $\omega_{\mathcal{T}}$.
- Linear mortars produce finer grids, especially in the two regions of high oscillation.

Continuous Measurement and Data Analysis for Reservoir Model Estimation

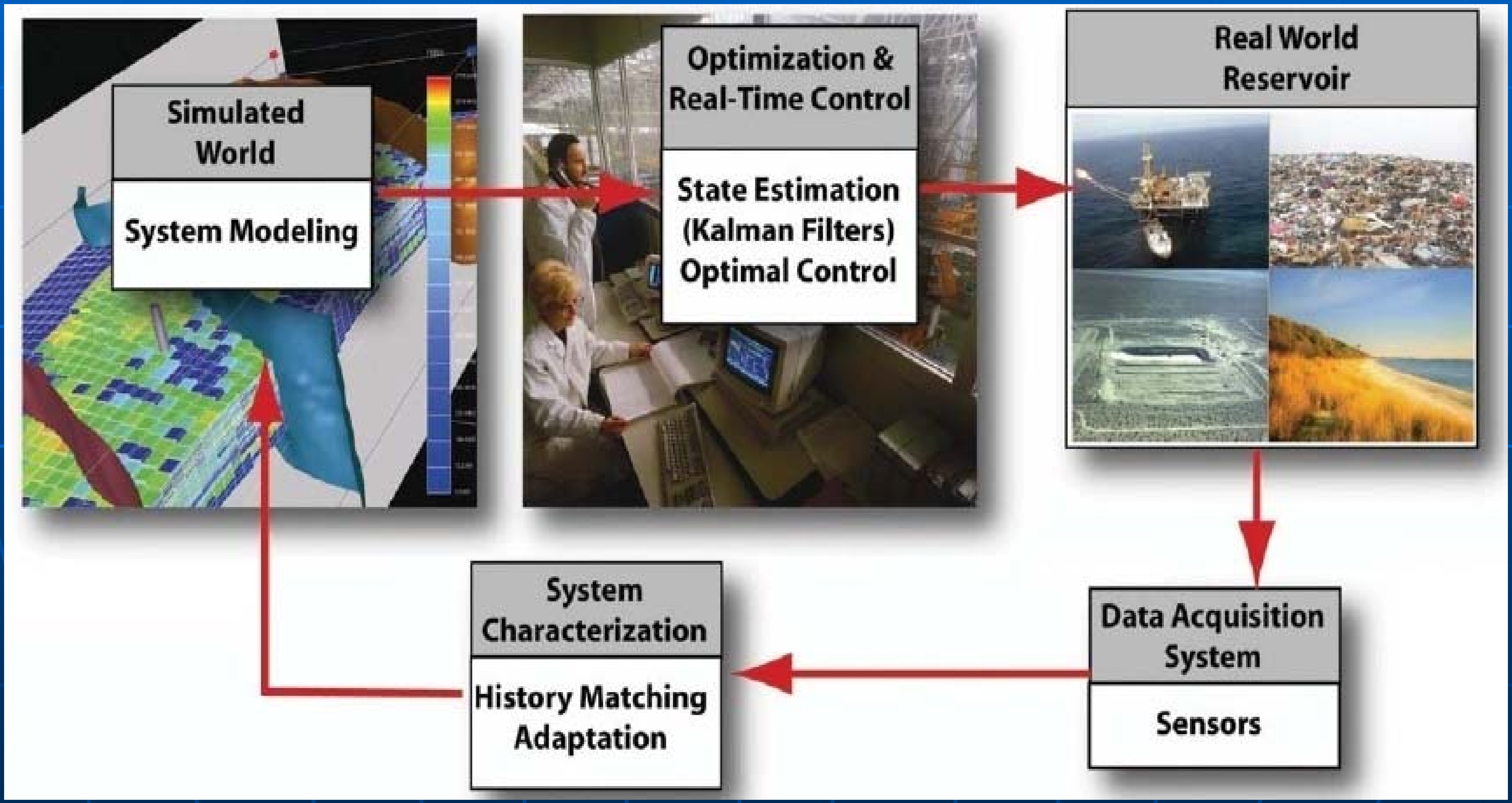

Source: E. Gildin, CSM, UT-Austin

Continuous Measurement and Data Analysis for Reservoir Model Estimation

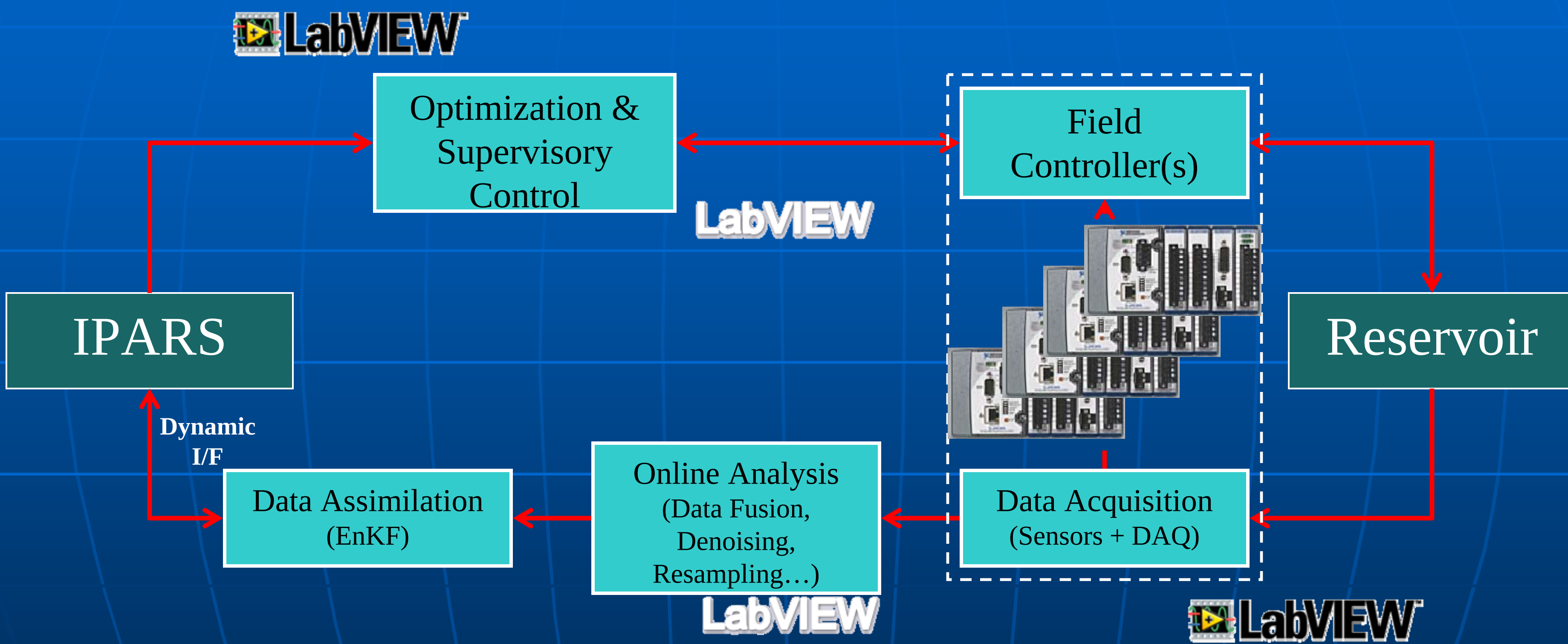

Source: I. Alvarado and D. Schmidt, NI

Parameter Estimation Using SPSA

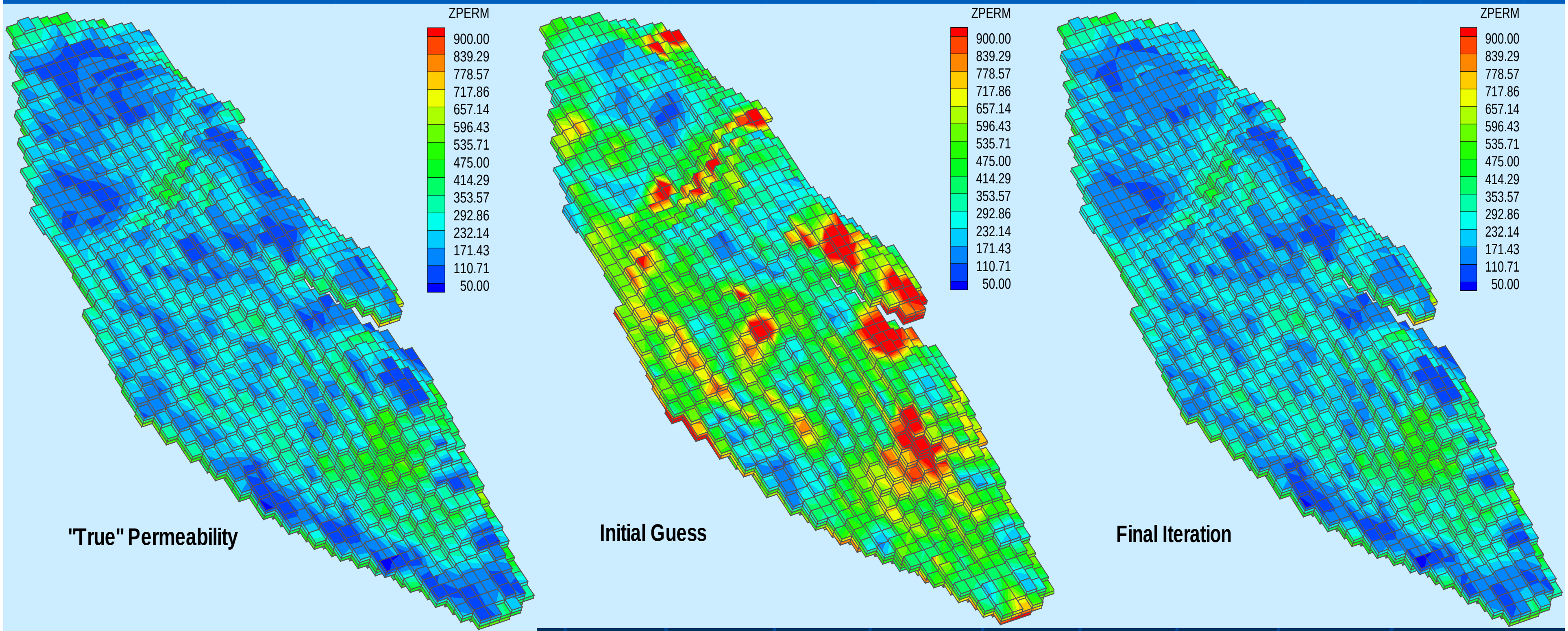

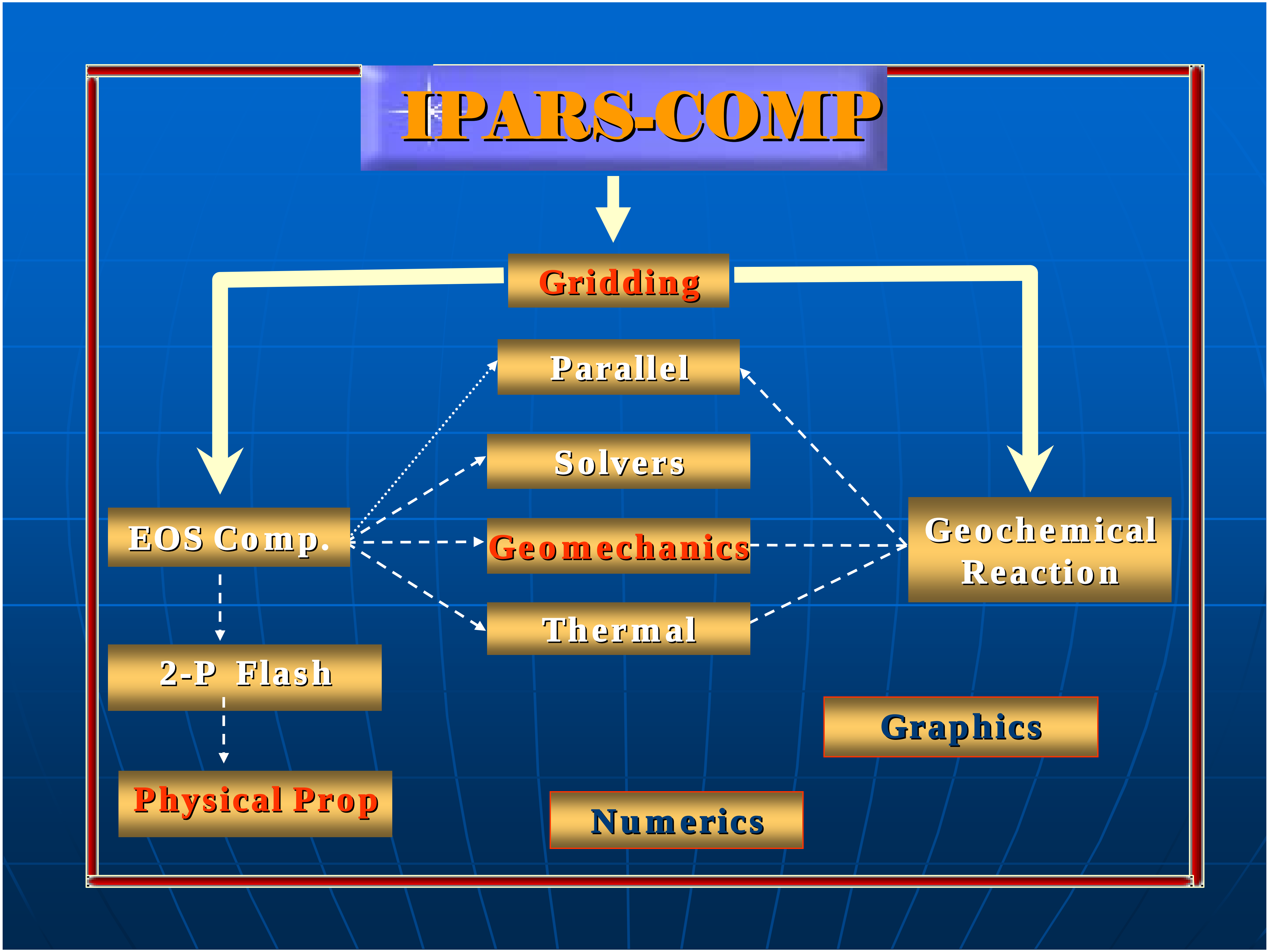
IPARS-COMP
Gridding
Parallel
Solvers
EOS Comp.
Geomechanics
Geochemical Reaction
Thermal
2-P Flash
Physical Prop
Graphics
Numerics

Center for Frontiers of Subsurface Energy Security
The University of Texas

Summary statement: Our goal is scientific understanding of subsurface physical, chemical and biological processes from the very small scale to the very large scale so that we can predict the behavior of CO2 and other byproducts of energy production that may need to be stored in the subsurface.

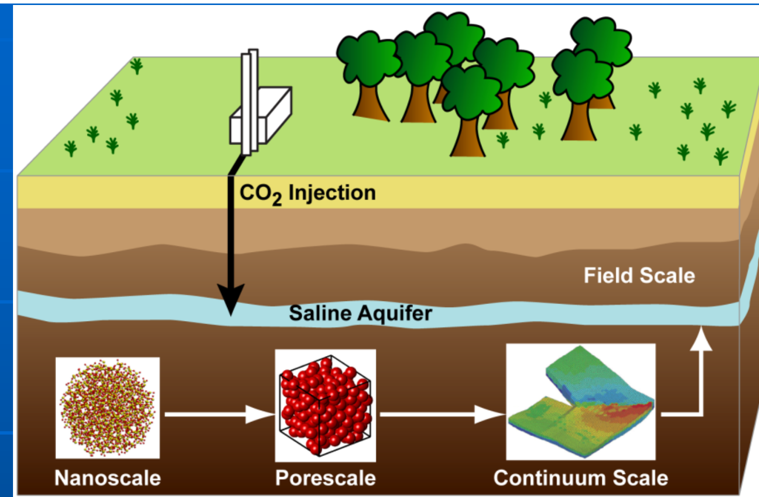

RESEARCH PLAN AND DIRECTIONS

- **Challenges and approaches**: Integrate and expand our knowledge of subsurface phenomena across scientific disciplines using both experimental and modeling approaches to better understand and quantify behavior far from equilibrium.
- **Unique aspects**: The uncertainty and complexity of fluids in geologic media from the molecular scale to the basin scale.
- **Outcome**: Predict long term behavior of subsurface storage.

an Office of Basic Energy Sciences
Energy Frontier Research Center

Conclusions

- Computational Science and Mathematics – Essential in Addressing Problems Impacting Energy and the Environment
    - Computation Required for Understanding and Developing Strategies for Energy Production, Carbon Capture and Storage, Storage of Nuclear Wastes and Renewables
    - Challenges Include MPP Modeling of Multiphysics, Multiscale Problems Accurately and Efficiently, and Incorporating Model Reduction, V&V and QU